# DEPARTMENT OF NATIONAL RESOURCES

# BUREAU OF MINERAL RESOURCES, GEOLOGY AND GEOPHYSICS



Record 1979/44

McARTHUR BASIN RESEARCH, MARCH QUARTER, 1979

K.A. Plumb (co-ordinator)

Record 1979/44

# McARTHUR BASIN RESEARCH, MARCH QUARTER, 1979

K.A. Plumb (co-ordinator)

CONTENTS



Figures

Figures (continued)



3

# McARTHUR BASIN RESEARCH

March Quarter 1979.

## PREFACE

All of the significant results and data resulting from the 1978 geological field work are summarised in this report, or in those for the September and December quarters (Plumb, 1979a, b). A special Field Work Report (e.g. Jackson & others., 1978) will not be produced this year.

This progress report also contains a reporting of the 1978 gravity survey, because quantitative interpretation, suitable for publication or for a special Record, is not possible until further field data have been collected during 1979.

## PRINCIPAL RESULTS

(1) Four geological papers have been completed for publication.

(2) 17 detailed stratigraphic sections are presented from the 1978 field work.

(3) Alternating lagoonal and more agitated shallow intertidal to supratidal environments are indicated for the Amelia Dolomite, in the southern McArthur Basin.

(4) A probable calcrete origin for 'oncolites' in the Amos Formation has been supported by preliminary petrography.

(5) A local provenance area to the southeast of the Abner Range is indicated during deposition of the Balbirini Dolomite. Depositional environments range from piedmont fans, through supratidal, to shallow subtidal environments.

(6) Dolomite concretions, found locally in the Barney Creek Formation, suggest that the Mallapunyah Fault may have acted as a channel-way for the circulation of mineralising brines.

(7) Five forms of distinctive columnar stromatolites have been described.

5

(8) Detailed gravity measurements have indicated near-surface sulphide mineralisation and buried stream channels.

(9) Preliminary quantitative modelling indicates the presence of density contrasts within the basin succession and implies an absence of major displacement across the Emu Fault.

## PUBLICATIONS

Papers on the following topics were completed and are now in press or about to go to press (see References):-

1. M.D. Muir (1979) has proposed a sabkha depositional model for a profile through the Mallapunyah Formation and Amelia Dolomite, of the McArthur Group, and has outlined its significance in the context of sulphide ore deposition.
2. M.D. Muir, D. Lock, & C.C. Von Der Borch (1979) have drawn precise analogies between sediments being deposited in the Coorong Lakes of South Australia and the Yalco Formation of the McArthur Group, and have applied the groundwater and evaporitic regimes of the Coorong to a model for the deposition of the Yalco Formation. Possible applications to the formation of sedimentary ore deposits are described.
3. M.R. Walter, I.N. Krylov & M.D. Muir (in prep.) have described distinctive columnar stromatolites from the McArthur Group and their palaeoecology.
4. Muir, Walter, & Jackson (1979), in a criticism of a paper by LaBarbera in Nature, point out the common occurrence of Metazoa in shallow-water and evaporitic sequences.

6

# GEOLOGY

M.J. Jackson (Task Leader), K.J. Armstrong, D. Gregg, I.N. Krylov, M.D. Muir, C.J. Simpson, M.R. Walter.

## SYSTEMATIC MAPPING (C.J. Simpson, M.J. Jackson)

Additional photo-interpretation has been carried out to fill in areas not completed during the 1978 field season. Preparation of the photoscale compilations was still in progress at 31 March, 1979.

## SEDIMENTOLOGICAL STUDIES (M.J. Jackson, M.D. Muir)

All the detailed stratigraphic sections which were measured during the 1978 field season have been summarised at a reduced scale, and are included in the report as Figures 3 to 19. Their locations are shown in Figure 1.

### Amelia Dolomite (M.J. Jackson)

Three well-exposed sections of Amelia Dolomite were measured in the southern part of the basin during the 1978 field season: two in the Kiana Dome area (Kilgour 78/5, 78/8) and one near Top Springs homestead (Kilgour 78/6). Summary logs have been prepared (Figs 10, 11, 13), following preliminary petrographic examination of thin sections, and some broad generalisations have been made on the depositional history of this unit in the southern area.

The base of the formation is marked, in all sections, by a distinctive stromatolite bioherm, 2 to 3 m thick, comprising convex domes (20 cm relief) at the base, grading up through pseudocolumnar to columnar, non-branching forms, into stratiform stromatolites at the top. This basal part of the Amelia Dolomite overlies a distinctly bedded shallow-water sandstone-siltstone sequence at the top of the Mallapunyah Formation. A marked reduction in the supply of terrigenous detritus, and possibly also a shallowing of water depth is indicated.

Throughout this southern area studied during 1978, the basal bioherm is succeeded by a laterally-uniform sequence, 60-70 m thick, of interbedded fine-grained dolarenites and dololutites which are characterised by regularly alternating stromatolite types. Bioherms of various types of Conophyton, 1 to 4 m thick (mean 2 m), alternate with intervals between 5 and 14 m thick (mean 8 m) containing domal and stratiform stromatolites, and thin layers of intraclast breccias and rare oolitic lenses. The synoptic relief on the stromatolites indicates deposition in very shallow water for most of this interval, and a regular migration back and forth of quiet lagoons over more agitated shallow intertidal to supratidal environments seems likely.

The rest of the Amelia Dolomite is everywhere dominated by intraclastic and oolitic dolarenites with rare stromatolites. In the east, this upper part is 60 m thick (Kilgour 78/5, 78/8) but in the west it is about twice as thick, and contains a significant amount of quartz sand. Except for the sand content, there is no apparent difference between the carbonate lithologies of the two areas, so the depositional environments were similar, except for the presence of an exposed land area supplying quartz detritus into the Top Springs area.

Amos Formation (M.D. Muir)

Preliminary petrography of thin sections of the structures from the Amos Formation, called 'oncolites' in the field, indicates that a calcrete pisolith origin is likely. Some of the pisoliths form around clasts, and some are overgrowths on multiple centres. Scattered, rounded quartz grains occur in the matrix, a feature which is also compatible with a calcrete origin. The original rock-type appears likely to have been a pebbly dolarenite, with varying proportions of quartz sand. Columnar-layered stromatolites have been found in a few stylolite-bounded fragments. The laminae are gently convex and columns vary from 1 to 2 cm across, up to 5 mm in synoptic height, and up to 6 cm in total height. Intercolumn spaces contain sandy dolarenite.

Balbirini Dolomite (M.D. Muir)

The distributions of the various facies have been plotted onto a generalised geological map around the Abner Range. At the northwestern end of the Abner Range, the Limmen Sandstone overlies the Dungaminnie Formation. The contact is always obscured by large amounts of scree from the Roper Group, but near McArthur River homestead extensive karstic weathering occurs in carbonate beds of the Dungaminnie Formation. Farther south, the Limmen Sandstone rests on progressively older beds of the Balbirini Dolomite until, in the southeastern part of the range, only the lowermost beds (from the *Conophyton*-complex downwards) are preserved.

The basal clastic unit of the Balbirini Dolomite varies from red shale and siltstone, in the north and west, to pebble conglomerate which is coarsest and thickest in the southeast. The conglomerate is locally derived and contains rounded pebbles and boulders of underlying rock units. The rounding of the pebbles appears to be a solution effect, related to pre-Balbirini karstic weathering of the underlying carbonate-rich formations. Small-scale solution features can be observed on the surfaces of some boulders. In the red shale-siltstone sequences of the northwest, thin lenses of pebble conglomerate occur at one or three levels. These contain a number of lithoclasts, and may represent the distal portion of the conglomerate spreads.

The implications of this distribution are that a topographic high must have existed to the southeast of the present outcrop, and conglomerates, possibly in the form of piedmont fans, spread north and west from a focal point to the south of Windy Gully. Some of the high ground at this time may have been related to upwards movement of Umbolooga Subgroup rocks, in the Mallapunyah Dome and other inliers to the south. Evaporite casts, in the form of discoidal gypsum casts and 'cauliflower cherts', occur in the red shale/siltstone sequence in the north and west, indicating deposition in the high supratidal zone, and suggesting that the subaqueous part of the depositional basin may lie farther to the north and west

Traces of evaporites become abundant in the overlying 130 m of section. These vary from halite casts and discoidal and prismatic gypsum casts, to 'cauliflower cherts'. Two pink 'tuffite' beds are believed to be claystones metasomatised by evaporite-derived potassium-rich brines. Rock types comprise red and purple shale and siltstone interbedded with cream and brown dololutite and dolarenite, which become more stromatolitic higher in this part of the section.

Some oolite beds are present in the upper part of the section and the sequence appears to indicate an overall transgression, from supratidal at the bottom to intertidal at the top. Evaporite relicts are more abundant in the northwest of the area than in the southeast. The unit mapped as the Conophyton-complex has recently been re-named the Balbirina prima bioherm series (Walter, Krylov, & Muir, in prep.) and this marks the end of the overall transgression.

Above the Balbirina prima bioherm series, a disconformity marks the beginning of a regression, and a sequence of intraclast breccia, dolarenite, dolomitic sandstone, and pure quartz sandstone follows. This sequence becomes gradually more dolomitic upwards, with stratiform stromatolites and Conophyton-like stromatolites, and culminates in the development of the 15-m thick Kussiella kussiensis biostrome. Because of pre-Limmen erosion, this biostrome has not been observed in the south and east of the area, but where it does occur it is of uniform thickness and appears to be made up of the same units in the same proportions. Because of its uniform and extensive distribution (the Kussiella biostrome has been recorded some 80 km northwest of the Abner Range) it appears likely that the stromatolites grew completely submerged in the depositional basin. No erosional features occur within or immediately above the biostrome. Intraclasts, oolites, domal stromatolites, and Conophyton characterise the upper 300 m of the Balbirini Dolomite, and these are all compatible with a submerged, probably subtidal, depositional environment.

With the evidence available at present, the distinction between a shallow-marine or large lake environment cannot be made. The evaporites in the lower part of the sequence indicate high groundwater salinity, but there is no evidence to show that the groundwater was marine. There are few evaporite remains above the Balbirina prima bed, and we have no indications of hypersalinity

\\

during deposition or diagenesis. There is some evidence of a topographic high to the south and east in the lower part of Balbirini Dolomite, but pre-Limmen erosion has removed any evidence from the higher parts of the section.

## MINERALISATION (C.J. Simpson)

Williams (1979) has recently discussed the significance of ferroan dolomite concretions around the H.Y.C. deposit. The concretions are oval, range from about 1 cm to 20 cm in diameter, and occur in dolomite-rich siltstones. Williams implies a direct genetic relationship between the development of the concretions and the introduction of the base-metals into the H.Y.C. deposit. He proposes that metalliferous brines flowed into the host sediments from the nearby syndepositional Emu Fault. In this model, the dolomite concretions assume new significance for exploration, since they may be indications both of base metal mineralisation and of fault zones which have acted as channels for brine movements.

During the 1978 field season, weathered silicified weakly-ferruginous concretions, identical in appearance to those at the H.Y.C., were identified in dolomites of the Barney Creek Formation some 65 km southwest of the H.Y.C. The locality (lat. $16^{\circ}47'$S, long. $135^{\circ}37'$E; Fig. 1) lies within the Mallapunyah Fault Zone.

While the Mallapunyah Fault has long been recognised as a major structural feature of the McArthur Basin, the presencce of the dolomite concretions would suggest, according to Williams' model,that it may also have acted as a channel-way for the circulation of mineralising brines. Mapping during 1978 (Plumb, 1979a) showed that the fault influenced sedimentation in the McArthur Group.

STROMATOLITE STUDIES (M.R. Walter, I.N. Krylov)

Dr. I.N. Krylov, of the USSR Academy of Sciences, worked in the BMR with the McArthur Basin Project throughout March, 1979.

Five forms of distinctive columnar stromatolites have been described from the Amelia Dolomite, Tooganinie Formation, Emmerugga Dolomite, and Balbirini Dolomite. Two are forms previously described from the Lower Riphean (1700-1350 m.y.) of the USSR: *Kussiella kussiensis* from the Balbirini Dolomite, and *Omachtenid omachtensis* from the Amelia Dolomite and Tooganinie Formation. A new form of *Acaciella* occurs in the Emmerugga Dolomite.

A newly described complex bioherm series, *Balbirina prima* (Walter & others., in prep), in the Balbirini Dolomite, is considered to have grown within a lagoon. Distinctive nodules of idiotopic dolomite in the lower part of the bioherm series are probably secondary after original anhydrite nodules. They are very similar to dolomite nodules in the H.Y.C. Pyritic Shale Member of the Barney Creek Formation.

*O. omachtensis* contains abundant acicular dolomite pseudomorphs after gypsum. It is apparent that these stromatolites originally consisted of gypsum and calcium carbonate - that is, they are primarily gypseous stromatolites, comparable to those known from Holocene lakes on Yorke Peninsula in South Australia.

## GEOPHYSICS

PALAEOMAGNETISM: M. Idnurm (Task Leader), J.W. Giddings.

No work has been carried out on McArthur Basin material during the March quarter, because of commitments to other projects, and it is anticipated that no work will be carried out during the June quarter.

MAGNETO-TELLURICS: D. Kerr (Task Leader), J.A. Major, A.G. Spence

Processing of measured data from the 1978 survey continued throughout the quarter, to remove 'noise' from the signals and to improve the quality of the data for input into the 2-D modelling. 2-D modelling was due to commence at the beginning of the June quarter.

GRAVITY: W. Anfiloff

Two long traverses and one short traverse, with a combined length of 185 km, were surveyed in the southern McArthur Basin during 1978 (Fig. 20). Traverses 1 and 2 crossed large areas of the Batten Trough and the Wearyan Shelf, and Traverse 3 crossed the H.Y.C. orebody. The final Bouguer gravity profiles are shown in Figures 21-24, and a quantitative interpretation along Traverse 1 is shown in Figure 21. The maximum variation in the gravity field encountered was 12 mGal, and the largest anomaly size was 10 mGal. The size of some of the important anomalies was less than 5 mGal.

Processing

Traverses 1 and 2 crossed more than 30 ridges. An advanced 2-D processing method enabled observations made over ridges to be reduced directly to Bouguer gravity values, without applying a separate terrain correction (Anfiloff & Flavelle, 1979). There was, therefore, no need to avoid steep topography during the survey and important gravity features were delineated more fully and accurately than they would otherwise have been. The largest terrain correction applicable was 0.8 mGal.

Comparison with helicopter reconnaissance data (BMR, 1976)

There are systematic and widespread discrepancies of 2-3 mGal, and local discrepancies of up to 5 mGal, between the existing helicopter reconnaissance data and the new data. This is to be expected, as the 11 km spacing reconnaissance coverage cannot detect anomalies whose width is half that amount. Moreover, there are indications that the reconnaissance survey precision in the McArthur Basin area is worse than the 1 mGal precision over most of Australia (Anfiloff et al., 1976). As the discrepancies are equal to the amplitudes of some of the main anomalies, the reconnaissance data cannot be used to define the boundaries of the Batten Trough, or the structural framework of the area generally. Nor can the detailed data be merged with the old data.

Interpretation

Important gravity features were delineated in the Emu Fault zone on all three traverses. Traverse 3 (Fig. 23) crossed the H.Y.C. orebody and detected an anomaly with a width of 6 km and an amplitude of 5 mGal. A similar anomaly was detected on Traverse 1 (Fig. 21), suggesting that the mineralised zone extends to the north along the Emu Fault. The gradients associated with this anomaly indicate a near-surface source, and the anomaly corresponds to a shallow mineralised body about 125 m thick, with a density contrast of 0.7 $g/cm^3$. The eastern flank of the anomaly is next to the fault scarp, where the terrain correction is 0.2 mGal.

On Traverse 2 (Fig. 22), there is a distinct transition between a smooth field in the east, and a more irregular field to the west. The transition does not coincide with the main topographic escarpment, as might be expected, and may denote another mineralised

15

zone. It coincides with a narrow ridge which requires a 0.8 mGal terrain correction. To have avoided this ridge would have obscured one of the main gravity features on this traverse.

Figure 21 shows a preliminary quantitative interpretation along the main traverse (Traverse 1). It is designed to convey the main constraints imposed by the gravity data on the analysis of the structure, and is therefore partly schematic. A more comprehensive interpretation will be produced after additional gravity coverage has been obtained in the 1979 field season.

Three sources of anomaly are identified. Firstly, there are very sharp, narrow gravity lows which must represent low-density bodies close to the surface. These are attributed to buried valleys filled with low density (1.9 $g/cm^3$) alluvium. Secondly, there is an abrupt, localised gravity high next to the Emu Fault. The steep gradients associated with this anomaly must represent a shallow dense body, and as indicated earlier, a body 125 m thick with a contrast of 0.7 $g/cm^3$ is implied.

The third source of anomaly is more ambiguous, because broader wavelengths are involved. The broad gravity low east of the Emu Fault could be caused by a broad basin, or by gradual lateral density changes in either the sediments or basement. At this stage, it is reasonable to assume a broad downwarp in basement. On the western side of the Emu Fault there are moderately broad anomaly features which must represent lateral density variations in the sedimentary section, probably caused by faulting. Two bodies with a density of 2.6 $g/cm^3$ are used to schematically represent mass excesses in the sediments resulting from faulting, and upfaulted basement is also assumed to contribute to the anomalies. The actual depth to basement cannot be reliably deduced from the broad anomalies without a detailed knowledge of densities, and a value deduced from geological mapping has been used at this stage. The computed attraction of the model without the substantial masking effect of the buried valleys is shown as a separate profile in Figure 21. It should be noted that there is good correspondence between fault anomalies and buried valley anomalies. This suggests that stream cannels developed along fault planes.

The limited size of anomalies generally suggests that density contrasts are not large, or that their cumulative effect is small. However, the anomalies associated with faults in the western part of Traverse 1 establish that there are some variations in density down through the sedimentary section, and possibly across the basement as well. Consequently, given the lack of any offset in gravity level across the Emu Fault, it is not possible to propose a major displacement across that fault. The fault's position near the top of a basement arch would favour dilation of the fault plane and the passage of mineralising fluids to form the dense shallow body.

More detailed modelling will be carried out, incorporating more precise expressions of the geological structures and alternative structural interpretations, after additional control is available from the 1978 M-T survey and from the 1979 gravity and seismic surveys.

## Conclusions

Irregular topography and buried valleys are a difficult combination, as both produce sharp gravity effects. These effects can be distinguished from each other, and from longer-wavelength components, only by measuring gravity in detail. The strategy used, of crossing elongate topography at right angles and reducing the data using an advanced processing method, has enabled these problems to be resolved successfully. As a result, the current survey has greatly added to the knowledge of structure in the area and has delineated a target for mineral exploration. The extensions of Traverse 1, planned for the 1979 field season, should provide more information on density contrasts, which can then be applied to the analysis of the whole traverse.

18

## REFERENCES

ANFILOFF, W., BARLOW, B.C., MURRAY, A.S., DENHAM, D., & SANFORD, R., - 1976 - Compilation and production of the 1976 Gravity Map of Australia. BMR Journal of Australian Geology and Geophysics, 1, 273-276.

ANFILOFF, W., & FLAVELLE, A.J., 1979 - Gravity interpretation over escarpments and in two dimensions generally. Geh formal interpretation method. Geophysics, 44, 371 (abstract).

BMR, 1976 - Gravity Map of Australia 1:5 000 000. Bureau of Mineral Resources, Canberra, Australia.

JACKSON, M.J., MUIR, M.D., PLUMB, K.A., LARGE, D.E., BROWN, M.C., & ARMSTRONG, K.J., 1978 - Field work report, McArthur Basin Project, 1977. Bureau of Mineral Resources, Australia, Record 1978/54 (unpublished).

MUIR, M.D., 1979 - A sabkha model for the deposition of part of the Proterozoic McArthur Group, and its implications for mineralisation. BMR Journal of Australian Geology and Geophysics, 4, 149-162.

MUIR, M.D., LOCK, D., & VON DER BORCH, C.C., 1979 - The Coorong-Model for penecontemporaneous dolomite formation in the middle Proterozoic McArthur Group, Northern Territory, Australia. In ZENGER, D.H. (Editor) - CONCEPTS AND MODELS OF DOLOMITIZATION - THEIR INTRICACIES AND SIGNIFICANCE. Special Publication, Society of Economic Palaeontologists and Mineralogists (in press).

19

MUIR, J.D., WALTER, M.R., & JACKSON, M.J., 1979 - Origin of the Metazoa. Nature ('Matters Arising'), 278, 580.

PLUMB, K.A. (Co-ordinator),1979a - McArthur Basin Research, September Quarter, 1978. Bureau of Mineral Resources, Australia, Record 1979/15 (unpublished).

PLUMB, K.A. (Co-ordinator),1979b - McArthur Basin Research Project Progress Report, December Quarter, 1978. Bureau of Mineral Resources, Australia,Record 1979/16 (unpublished).

WALTER, M.R., KRYLOV, I.N., & MUIR, M.D., in prep. - Carpentarian (Middle Proterozoic) stromatolites from the McArthur Basin and Mount Isa region, Australia. Alcheringa.

WILLIAMS, N., 1979 - The timing and mechanisms of formation of the Proterozoic stratiform Pb-Zn and related Mississippi Valley-type deposits at McArthur River, N.T., Australia. Society of Economic Geologists-American Institute of Mining Engineers Joint Meeting, New Orleans, Preprint No. 79-51.

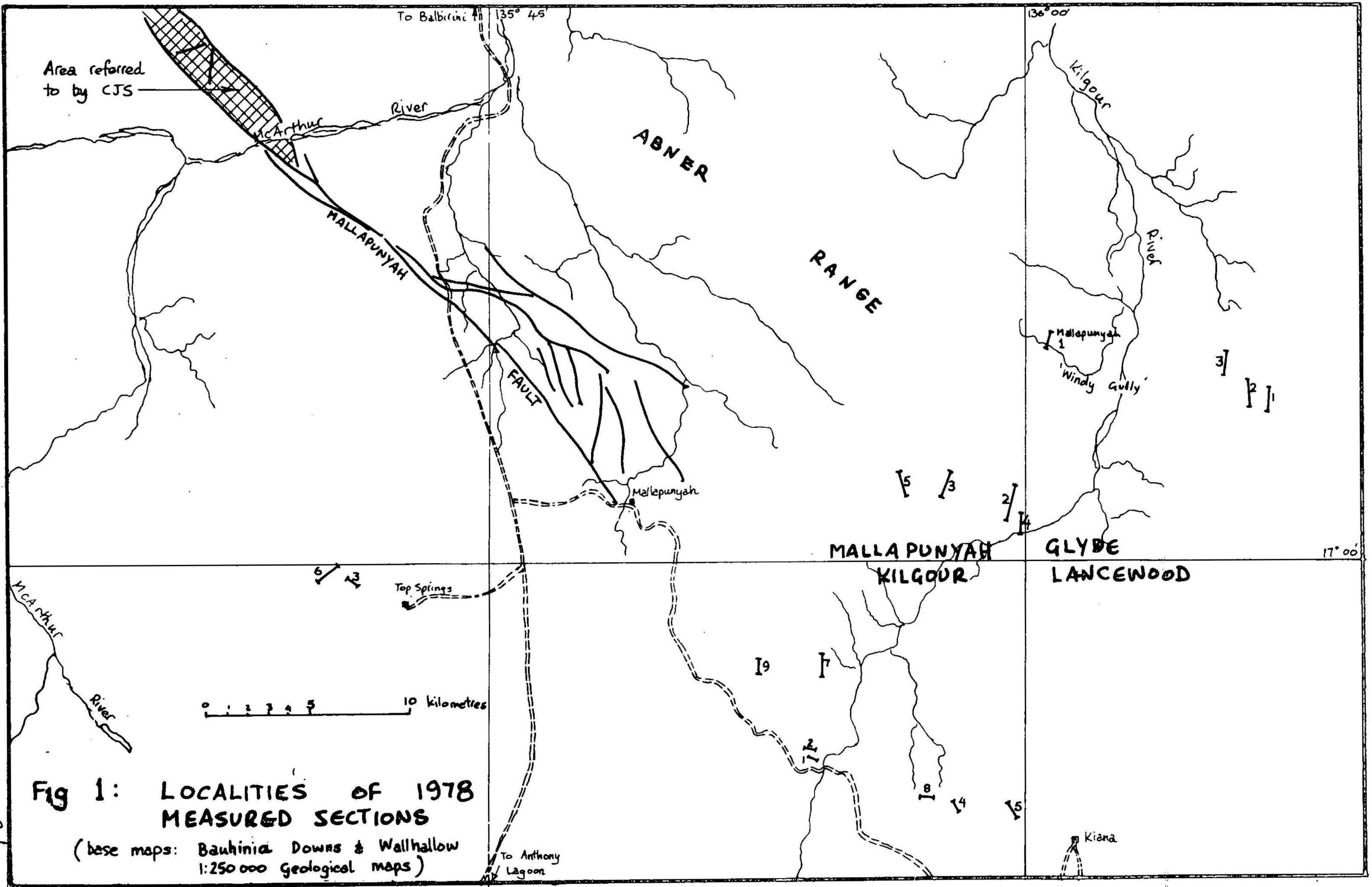


Fig 1: LOCALITIES OF 1978 MEASURED SECTIONS

(base maps: Bauhinia Downs & Wallhallow 1:250 000 Geological maps)

## SYMBOLS

### Lithology

- Conglomerate
- Dolomitic coarse sandstone
- Coarse Sandstone
- Sandy dololutite
- Fine sandstone
- Siltstone
- Mudstone or shale
- Interbedded siltstone & Dololutite
- Silcrete
- Chert in shape of Conophyton
- Chert
- Calcrete
- No exposure
- Recrystallised dolostone
- Dolarenite
- Dololutite

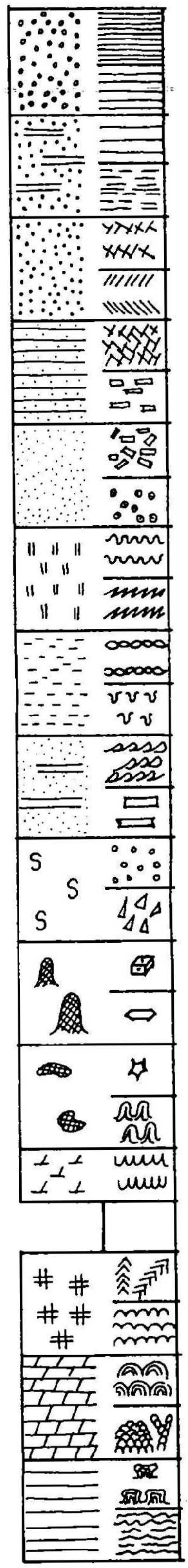

### Sedimentary Structures

- Laminated to thin bedded (Wavy if bedding is wavy)
- Medium bedded
- Thick bedded
- Discontinuous bedding
- Cross stratification/bedding
- Fine scale cross stratification/bedding
- Large scale cross stratification/bedding
- Intraclasts sub-parallel to bedding
- Intraclasts and disorganised flakes (usually called flake breccia)
- Oolites
- Symmetrical ripples
- Asymmetrical ripples
- Lenticular bedding
- Load casts
- Slumping
- Tuff
- Concretions
- Breccia
- Halite cast
- Gypsum cast
- Desiccation cracks
- Teepee structures
- Cuspate stromatolites
- No esposure
- Vertical and inclined Conophyton
- Low small domes
- Steeper larger domes
- Columnar and branching columnar stromatolites
- Domes with overturned sides
- Algal lamination or stratiform stromatolites

FIGURE 2. SYMBOLS USED IN SUMMARY LOGS OF THE MEASURED SECTIONS, 1978.

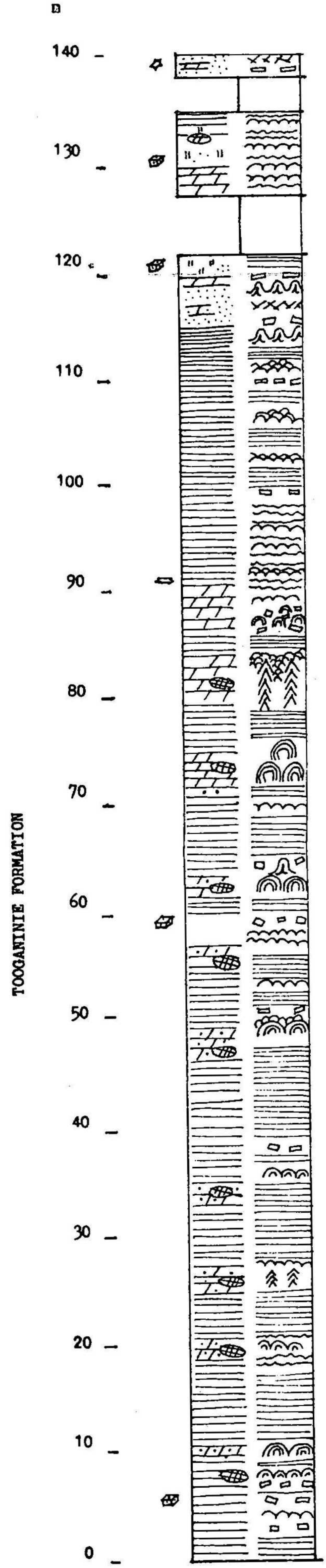


Cross-bedded coarse dolomitic sandstone.
Intraclast breccia. Mud-cracked.

Domal and stratiform stromatolites.

Thin-bedded red siltstone with halite casts.
Domal and stratiform stromatolites.

Silcrete rubble.

Thin-bedded siltstone with halite casts.
Teepee structures followed by angular flake breccia and low-angle cross-bedded quartz sandstone.

Dolomitic shale with some domal stromatolites.

Domal and stratiform stromatolites.

Gypsum pseudomorphs.

Domal stromatolites with intraclasts between domes.

Very large <u>Conophyton</u> with small cuspate stromatolites between columns.

Large domal stromatolites.

Domal stromatolites

Dolomitic shale.

Large domal stromatolites. Teepees between domes.

Halite casts in dololutite intraclasts.
Small domal stromatolites.

Small domal stromatolites.
Dolomitic shale.
Large domal stromatolites with small domes on top.

Dolomitic shale.

Domal and stratiform stromatolites.

Dolomitic shale.

Inclined <u>Conophyton</u>. Small domes on top.

Dolomitic shale.
Domal and stratiform stromatolites.

Dolomitic shale.

Domal stromatolites and intraclasts. Halite casts.

Dolomitic shale.

FIGURE 3a GLYDE 78/1 (1)

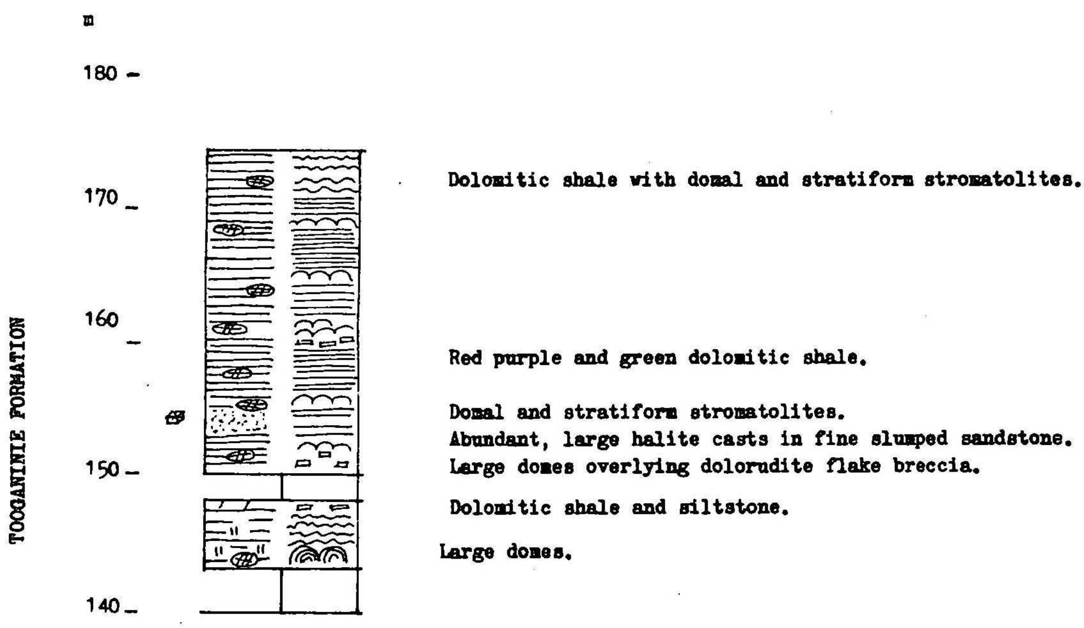


FIGURE 3b OLYDE 78/1.(2).

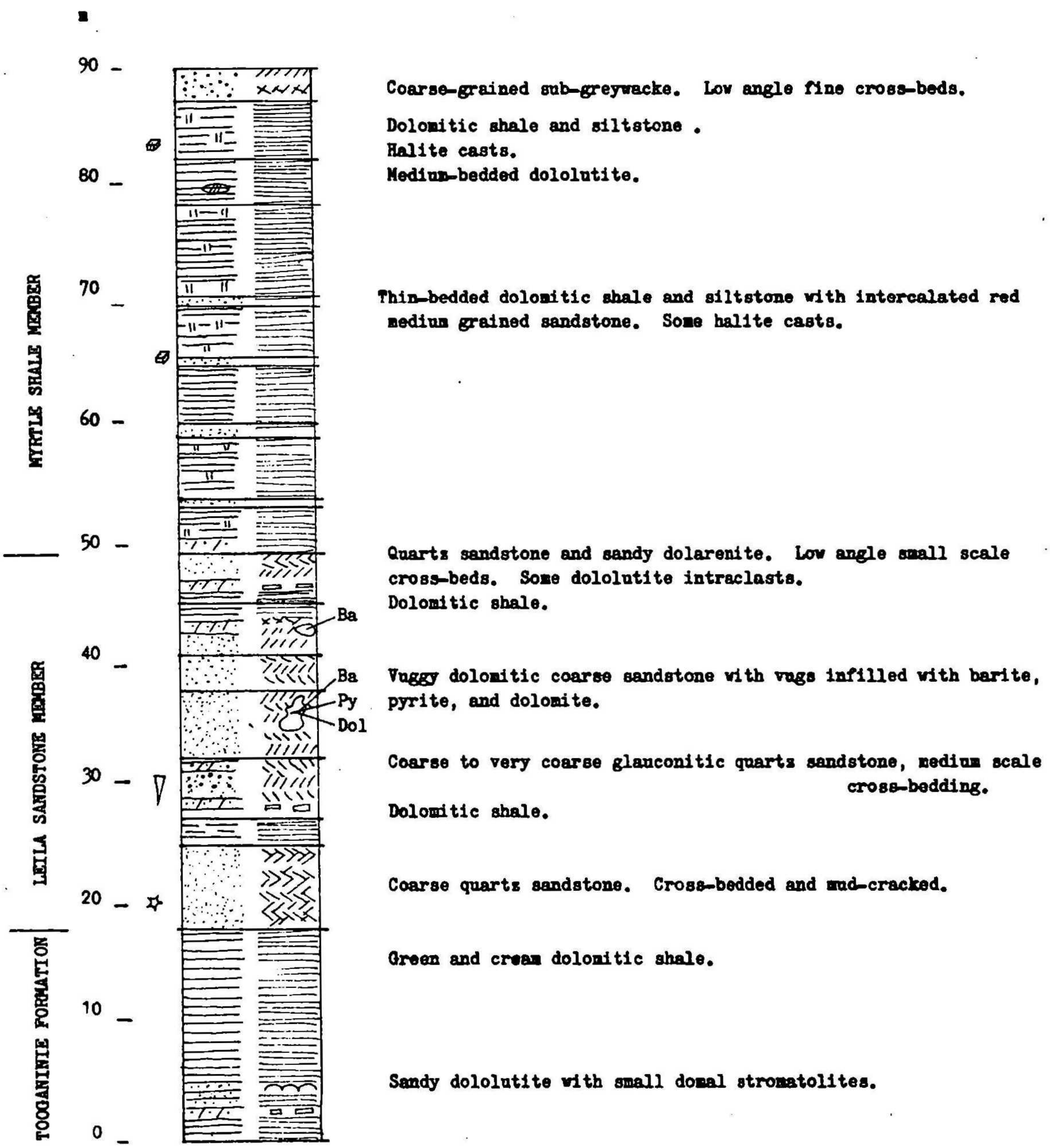


FIGURE 4 GLYDE 78/2.

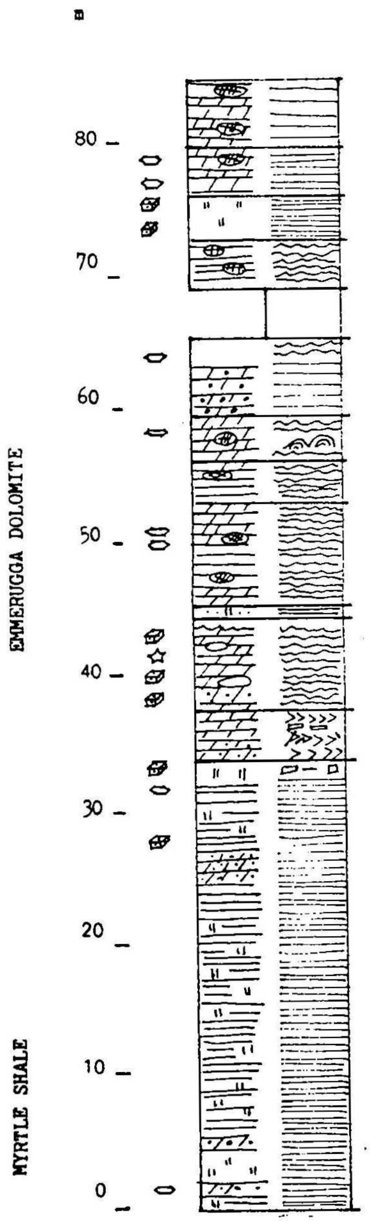


Massive dolarenite with laminar and nodular chert.

Prismatic gypsum casts in flat-bedded sparry dolarenite.

Halite casts in thin-bedded red siltstone.

Dololutite with stratiform stromatolites.

Prismatic gypsum pseudomorphs.

Thick-bedded dolorudite breccia.

Abundant prismatic gypsum casts. Domal and stratiform stromatolites.

Abundant prismatic gypsum casts.

Dark red fine sandstone and siltstone.

Dark red shale and siltstone with halite casts, interbedded with dololutite with abundant halite casts and saccharoidal chert. Stratiform stromatolites and mud-cracks.

Ferruginous cross-bedded sandy dolarenite.

Halite casts overlying prismatic gypsum casts.

Halite casts.

Red and purple shale and siltstone, with occasional thin dolorudite beds.

? Anhydrite casts.

FIGURE 5 GLYDE 78/3

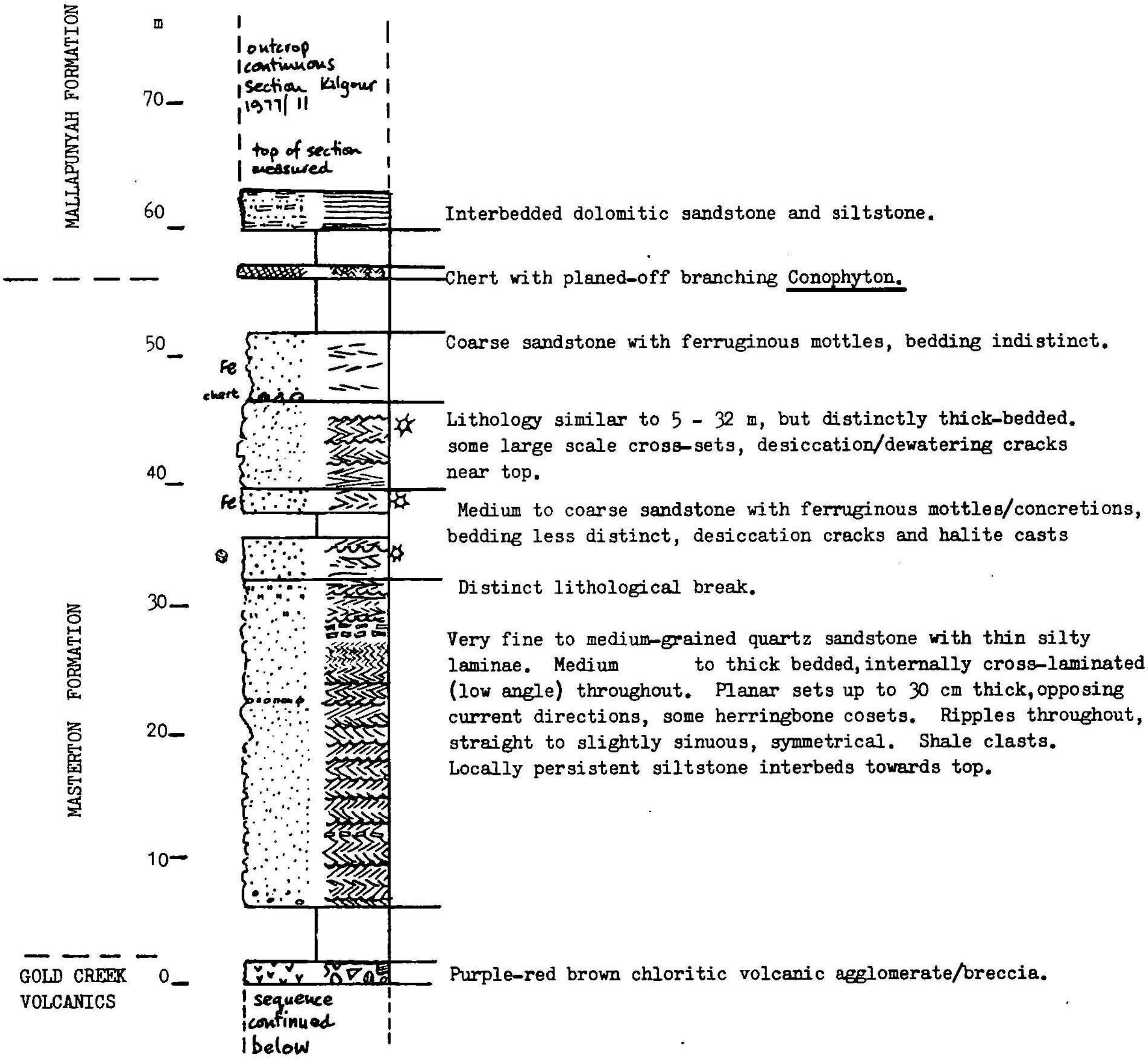


FIGURE 6 KILGOUR 78/1

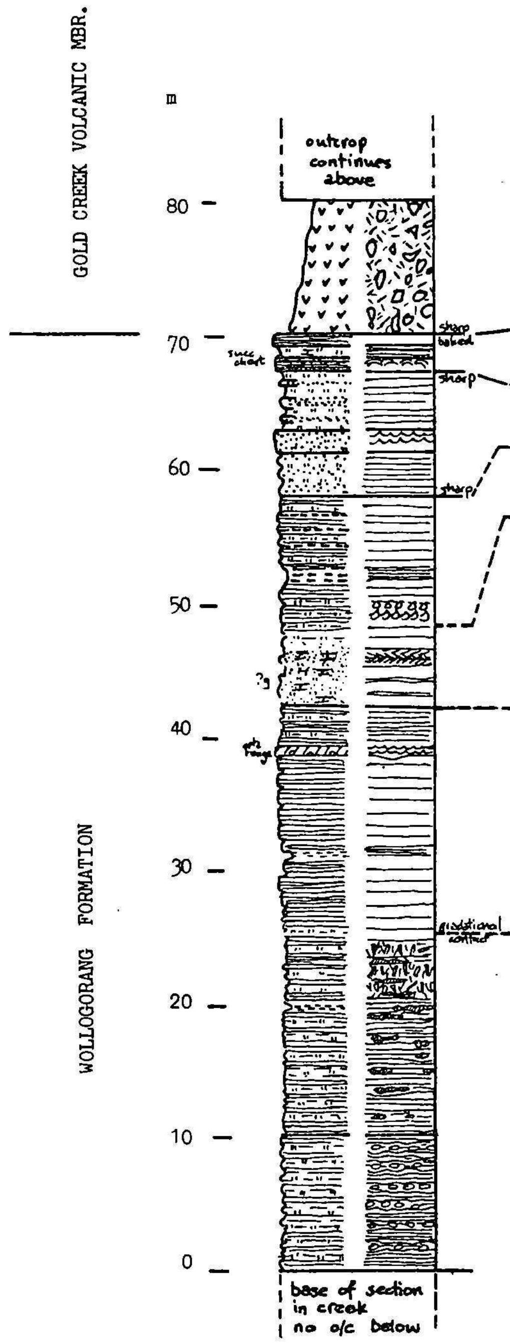


Volcanic agglomerate

Two tan hard dololutite beds separated by silt bed.
Succrosic chert laminae and domal stromatolites in lower bed.
Interbedded dolomitic siltstone/shale and dolomitic sandstone, ?glauconitic. Medium quartz sandstone with ripples at 62-63m.

Thinly interbedded silty dololutite and shale: slumping, loading, ball and pillow structures near base.

Thinly interbedded dolomitic fine sandstone and siltstone/shale. Thick, cross-stratified and rippled black sandstone at 47-48 m. ? glauconite.

Thin to medium distinctly bedded dark grey to brown weathering dololutite, rare shaley partings. Dololutite bed with erosive base and quartz and chert infilled vugs at 38 m. Silty laminated interval at top.

Edgewise flake breccia

Thin bedded to laminated dark grey to black silty dololutite:

Chert nodules.

Organic-rich ovoids.

FIGURE 7 KILGOUR 78/2

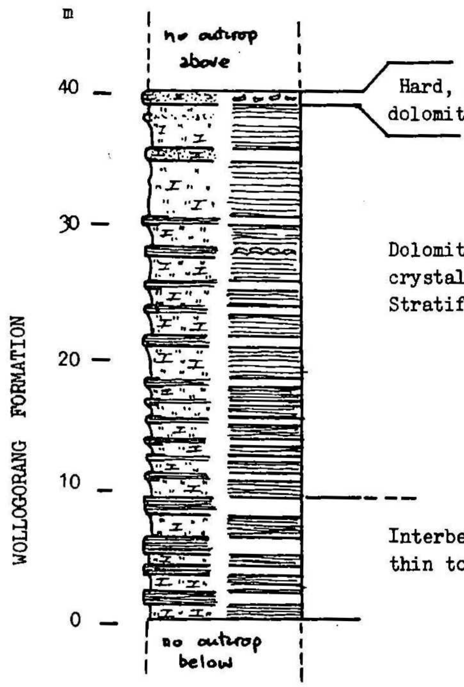


Hard, very fine grained dolomitic sandstone interbedded with dolomitic siltstone. Red shale intraclasts at 39 m.

Dolomitic siltstone or shale with interbeds of harder crystalline dolostone (5 to 20 cm thick).
Stratiform stromatolites in 10 cm thick biostrome at 28 m.

Interbedded hard dolostone and dolomitic siltstone, thin to medium bedded, some wavy laminations.

FIGURE 8 KILGOUR 78/3

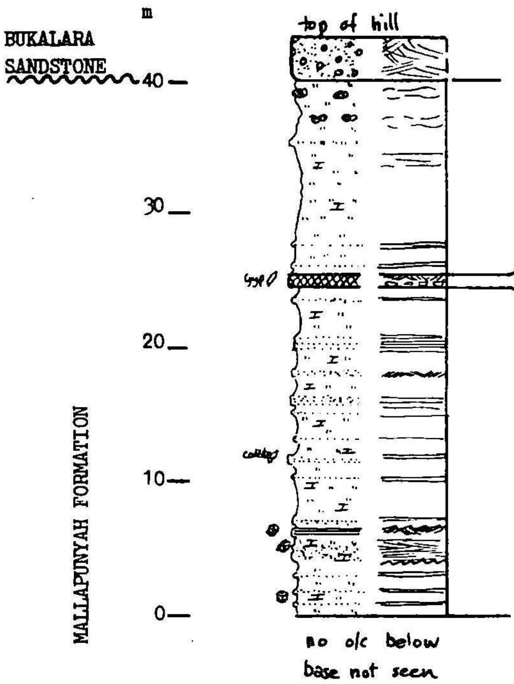


Conglomeratic coarse angular sandstone.

UNCONFORMITY

Mainly dolomitic siltstone with rare sandstone interbeds, small nodular cherts and cauliflower cherts near top.

White chert marker bed with gypsum pseudomorphs. Chert replaces dolostone bed with intraclasts, ripples, and cross-laminae.

Red-brown dolomitic siltstone with thin (few cm) sandstone interbeds (rarely cross-stratified).

Halite casts common near base (skeletal forms in thin dololutite at 7 m).

FIGURE 9 KILGOUR 78/4.

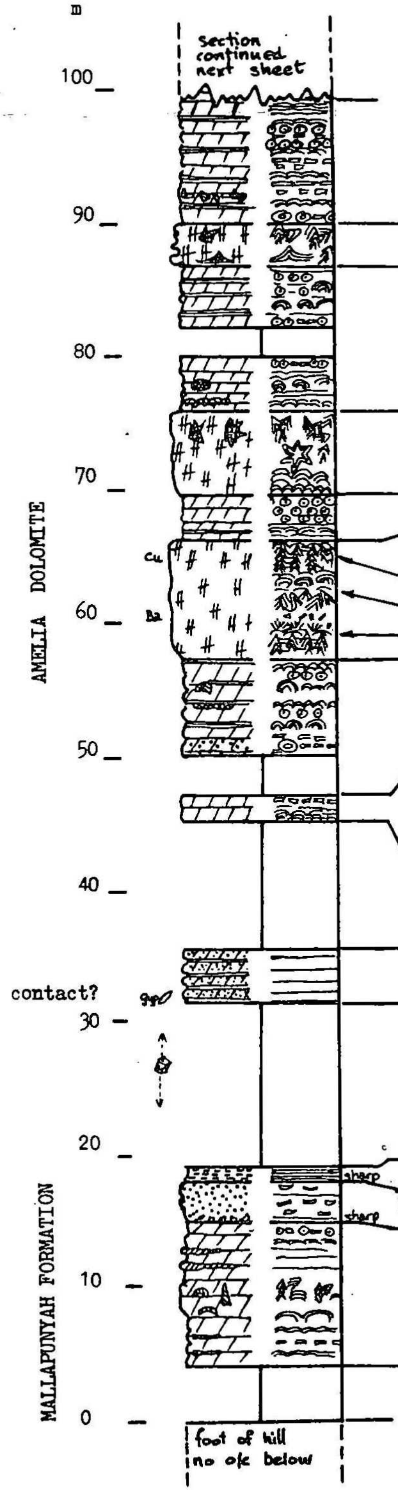


Oolitic and intraclastic dolarenite with thin interbeds of dololutite low domal and stratiform stromatolites. Oncolite bed at base, intraformational conglomerate at 92 m.

Recrystallised dolostone with branching Conophyton partially replaced by chert.

Oolitic and stromatolitic dolarenite with dololutite interbeds.

Massive recrystallised dolostone with chert replacement of stromatolites: star-shaped Conophyton stromatolites capping domal stromatolites.

Oolitic dolarenite capping dololutite low domal stromatolites.

Massive recrystallised dolostone with stromatolite series shown:
Ridged Conophyton.
Low domes with branching Conophyton below.
Intraclast breccia on low domes, ridged Conophyton below.

Stromatolitic dololutite interbedded with dolarenite (oolitic), low flat domes and hemispherical forms (relief 15 cm).
Intraclast conglomerate with oncolites at base.

Stromatolitic dolarenite, stratiform to pseudocolumnar laterally-linked forms, capped by intraclastic dolarenite.

Medium interbedded coarse sandy dolarenite and dololutite.
Gypsum pseudomorphs.

No exposure, siltstone and sandstone scree with halite casts.

Purple siltstone and shale.
Ferruginous coarse grained quartz sandstone, clay clast impressions.

Stromatolitic dolarenite, stratiform, domal and branching Conophyton stromatolites, replaced by chert, oolites and intraclasts at top.

FIGURE 10a KILGOUR 78/5(1).

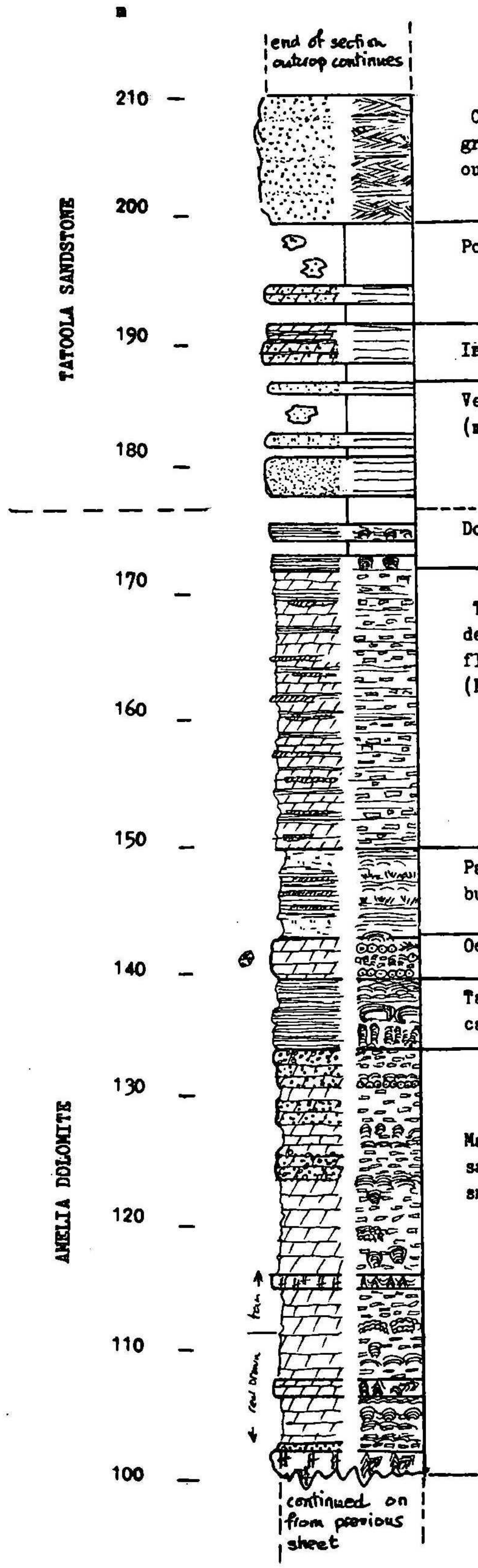


Coarse-grained quartz sandstone with interbeds of flaggy fine-grained sandstone. Low angle planar cross-stratification. Weathered-out carbonate grains/clasts common.

Poor outcrop of fine-grained sandstone and purple silty dolostone.

Interbedded dololutite and dolomitic fine grained silty sandstone.

Very fine-grained glauconitic quartz sandstone, flaggy thin bedding (minor dolomitic silty interbeds).

Dololutite with large domes.

Thin bedded to laminated dololutite and dolarenite commonly intraclastic developing to conglomeratic: dark grey chert in thin beds common. Abundant float of dolomitic silt suggests silty interbeds present. (Poor exposure).

Parallel laminated dololutite, dark chert laminae, poorly developed bulbous stromatolites. Thin edgewise flake breccia beds.

Oolitic dolarenite and stromatolitic dololutite, large domes at top.

Tan dololutite with bioherm series of columnar laterally linked stromatolites capped by large domes capped by stratiform stromatolites. Some dolarenite infillings.

Mainly intraclastic dolarenite with beds of Conophyton and conglomeratic sandy beds near top. Solitary columnar stromatolites and mounds of small pseudocolumnar stromatolites present.

FIGURE 10b KILGOUR 78/5 (2).

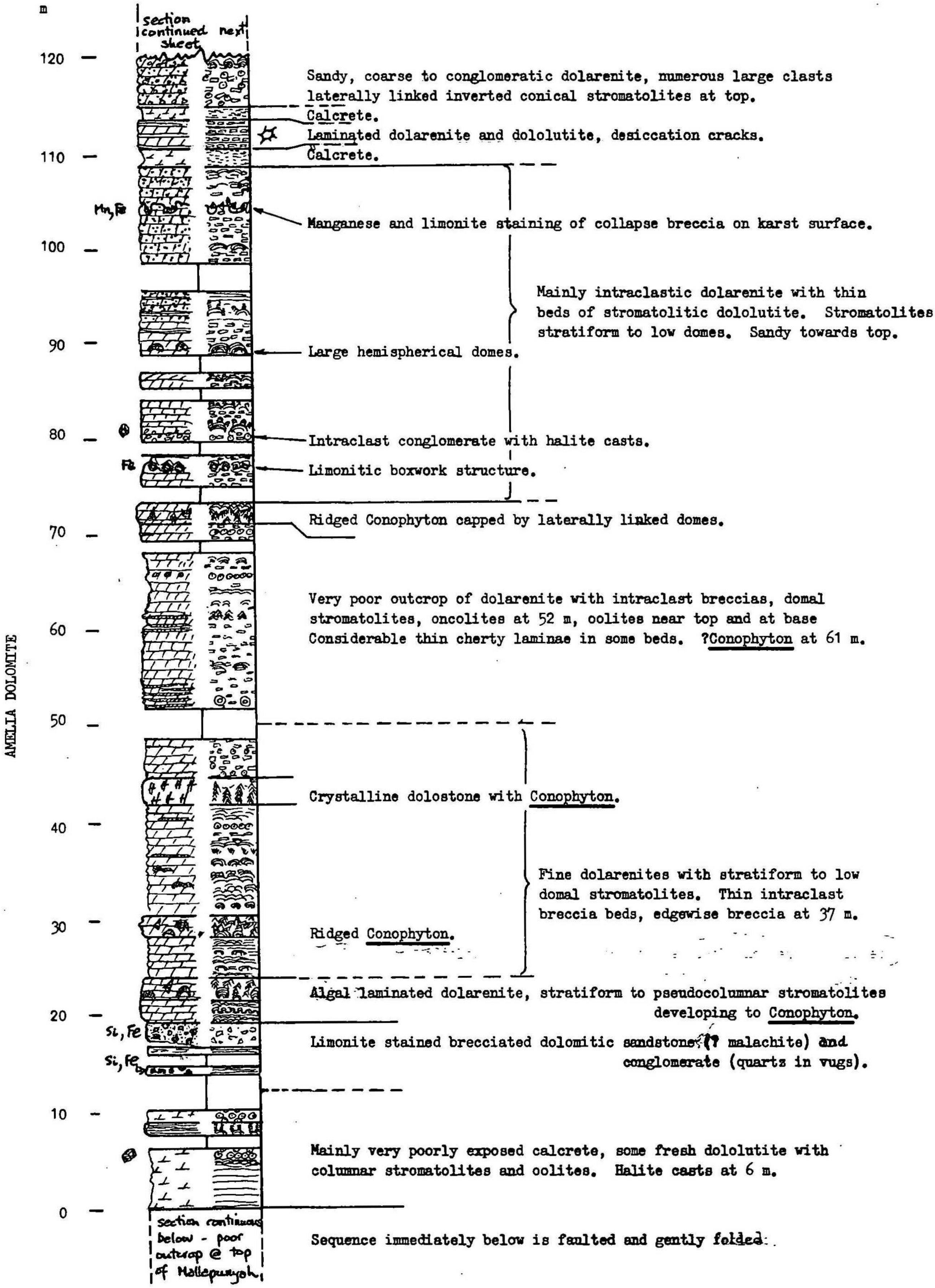


33

FIGURE 11a KILGOUR 78/6 (1).

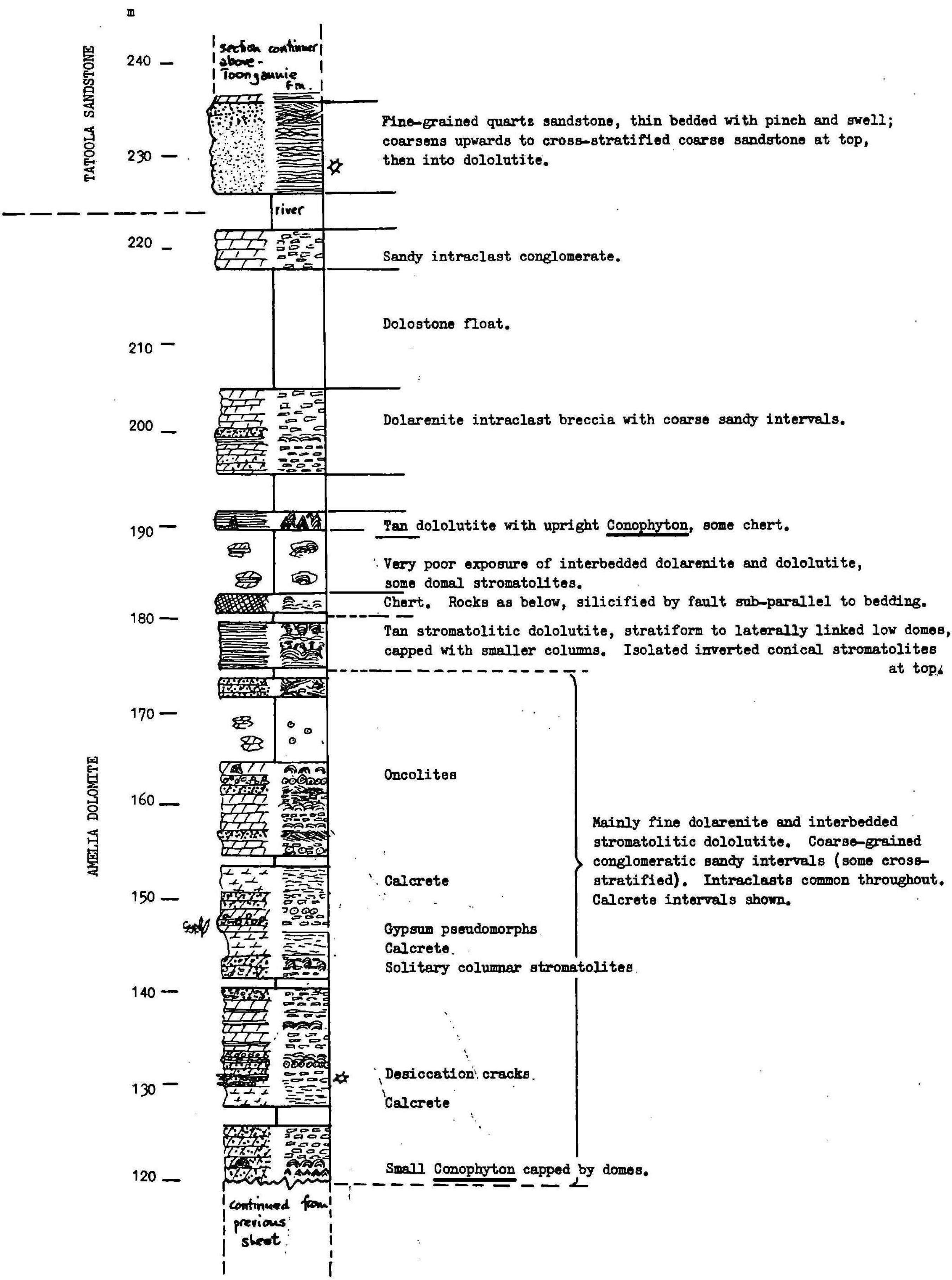


FIGURE 11b KILGOUR 78/6 (2).

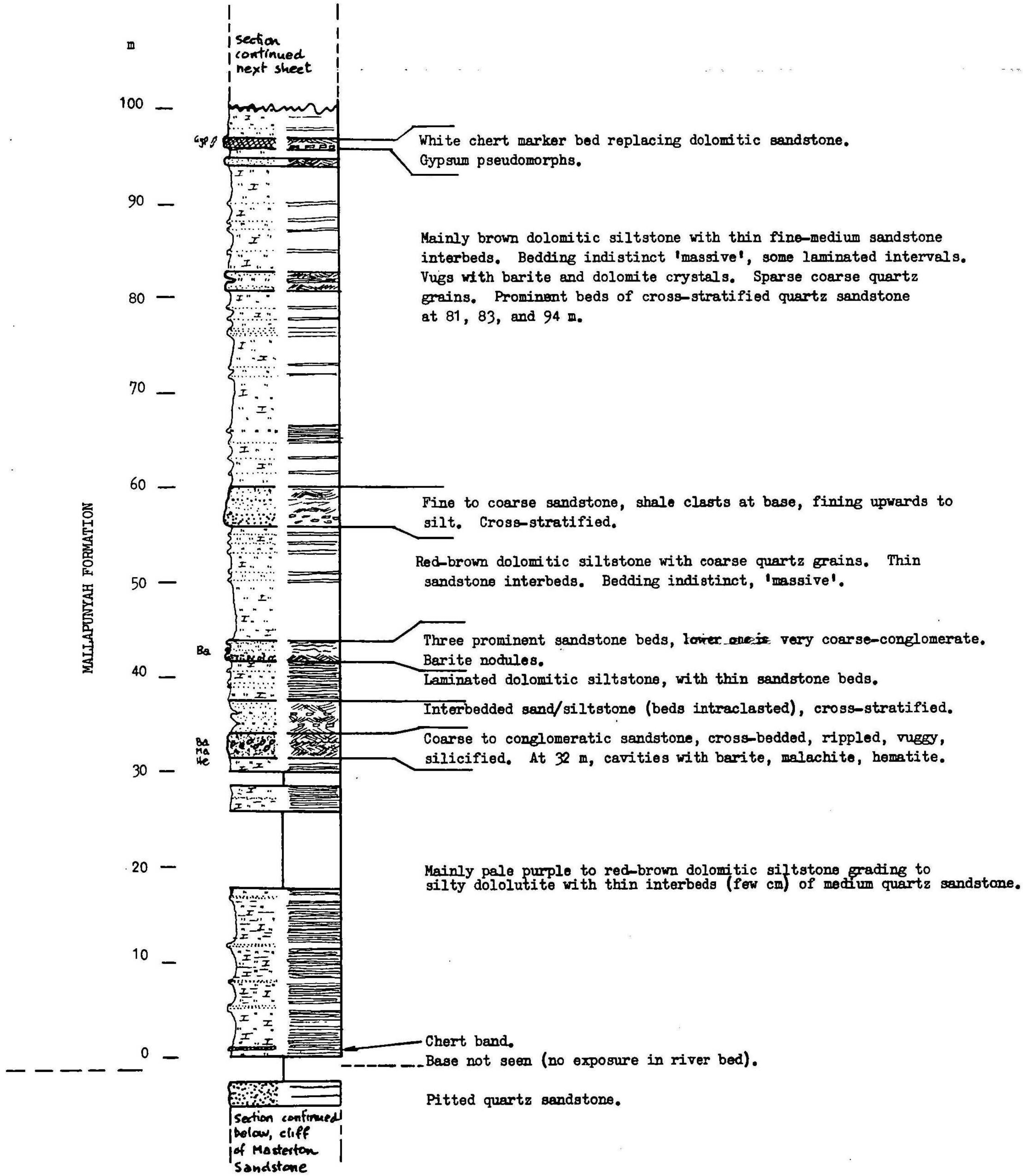


FIGURE 12a KILGOUR 78/7 (1).

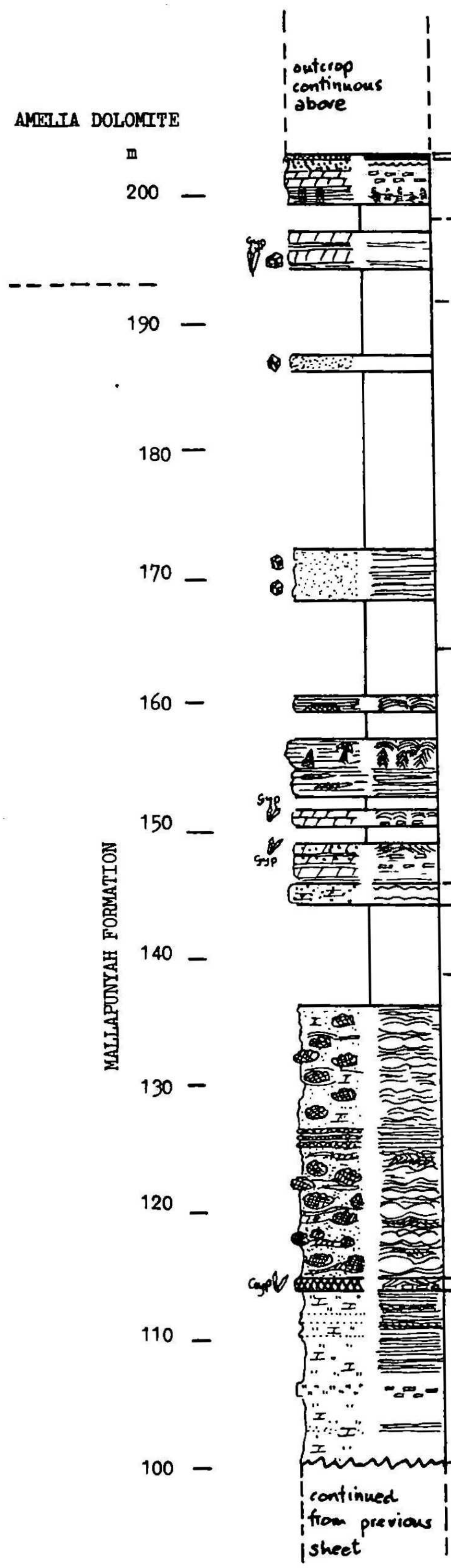


Green chert bed.
Coarse rippled sandstone, capping flake breccia beds capping bioherm of pseudocolumnar stromatolites.

Dololutite and dolarenite with gypsum and halite casts.

Poorly exposed fine grained sandstone with halite casts.

Interbedded dolarenite and dololutite (commonly chertified) with domes and Conophyton. Gypsum pseudomorphs in sandy cross-laminated dolarenites.

Rippled, friable dolomitic sandstone.

Fine to medium dolomitic sandstone, some intraclasts of dolostone, flame structures, and cross-stratification.
Cauliflower chert nodules throughout (pushing apart bedding), laterally persistent chert beds after sandstone at 125 m.

White chert marker bed with clasts at base and cross-laminae at top. Gypsum pseudomorphs.

Mainly brown dolomitic siltstone with interbeds of sandstone. Distinctly laminated and sandy near top (some ripple drift).

FIGURE 12b KILGOUR 78/7 (2).

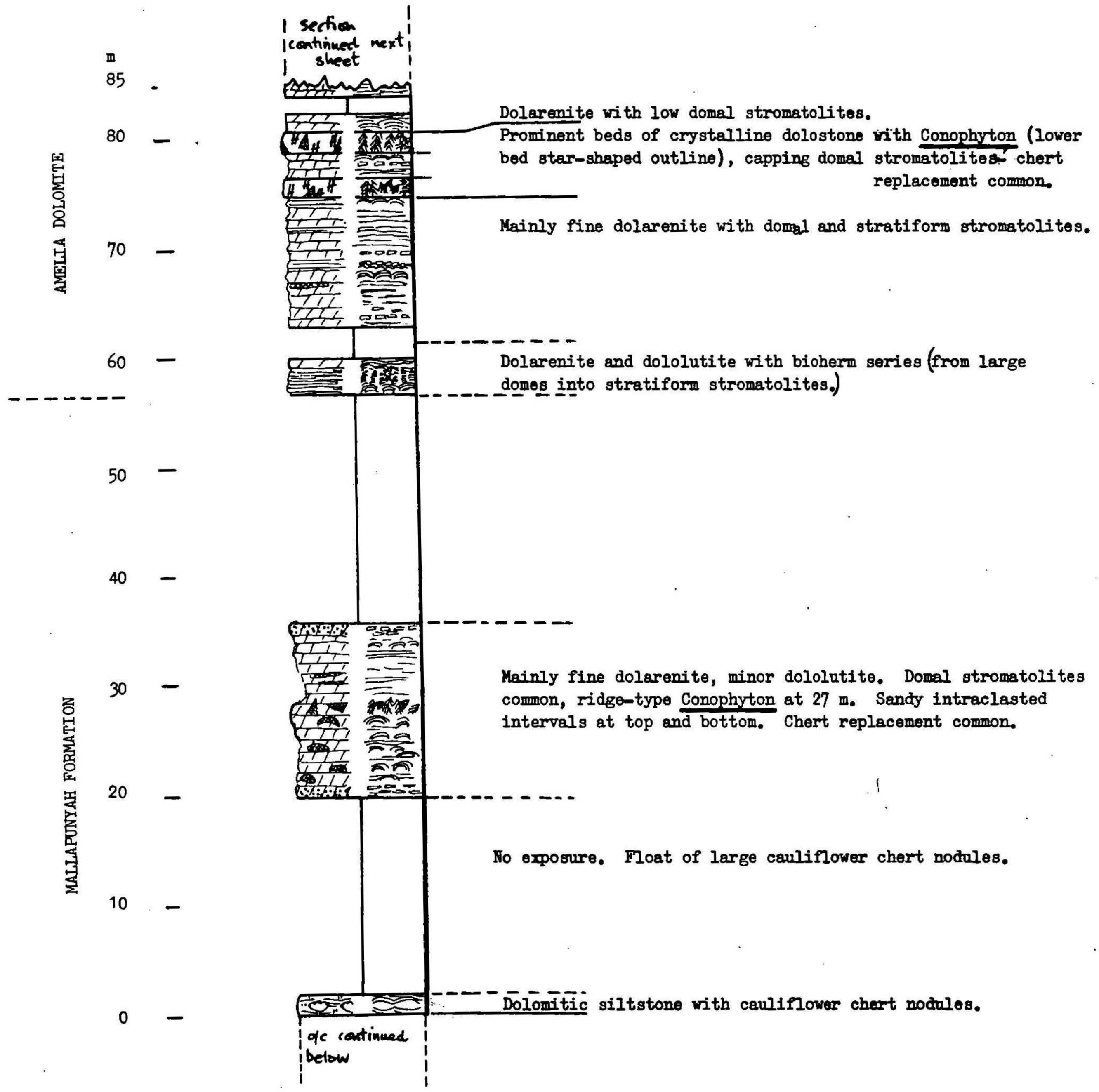


FIGURE 13a KILGOUR 78/8 (1).

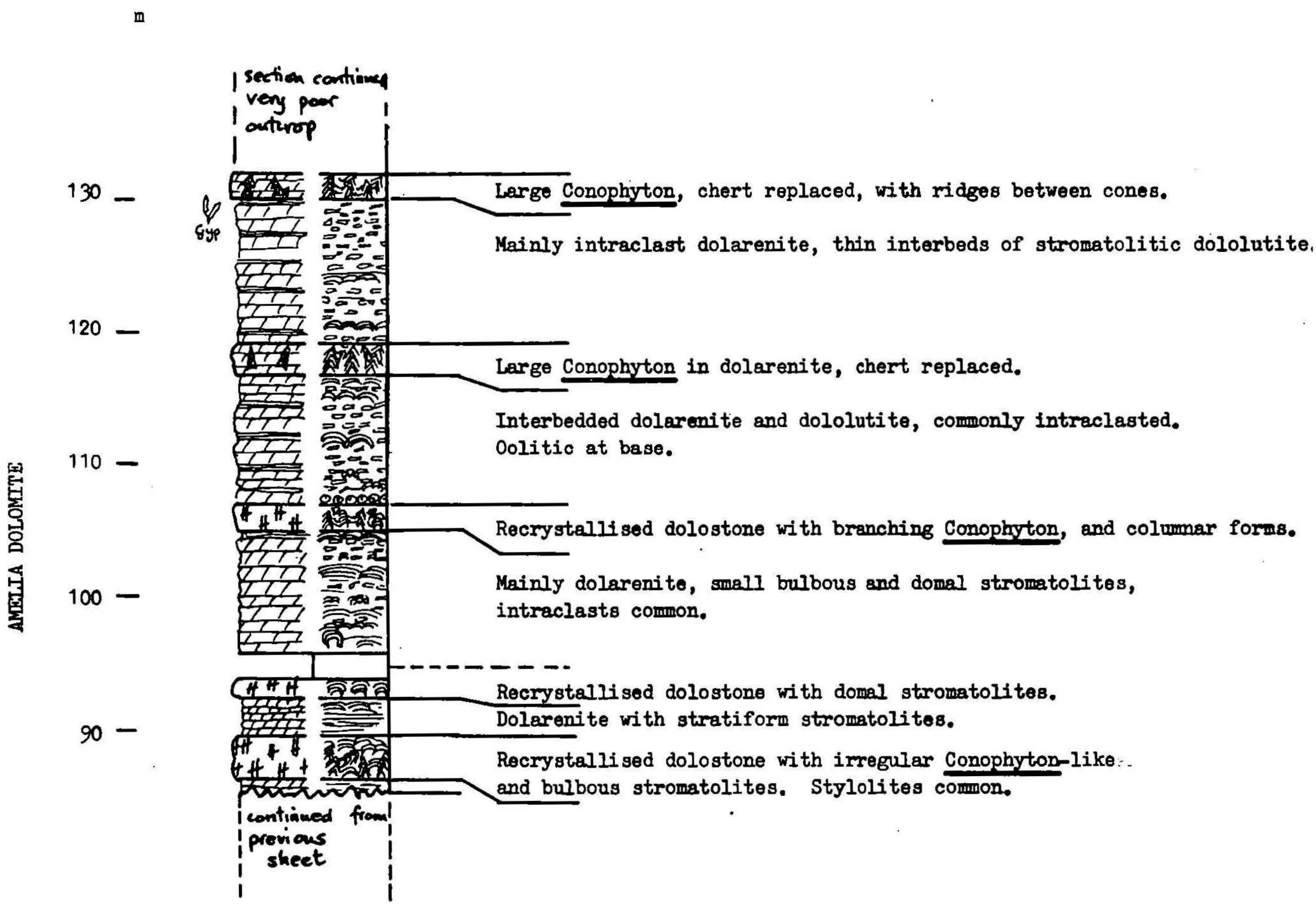


FIGURE 13b KILGOUR 78/8 (2).

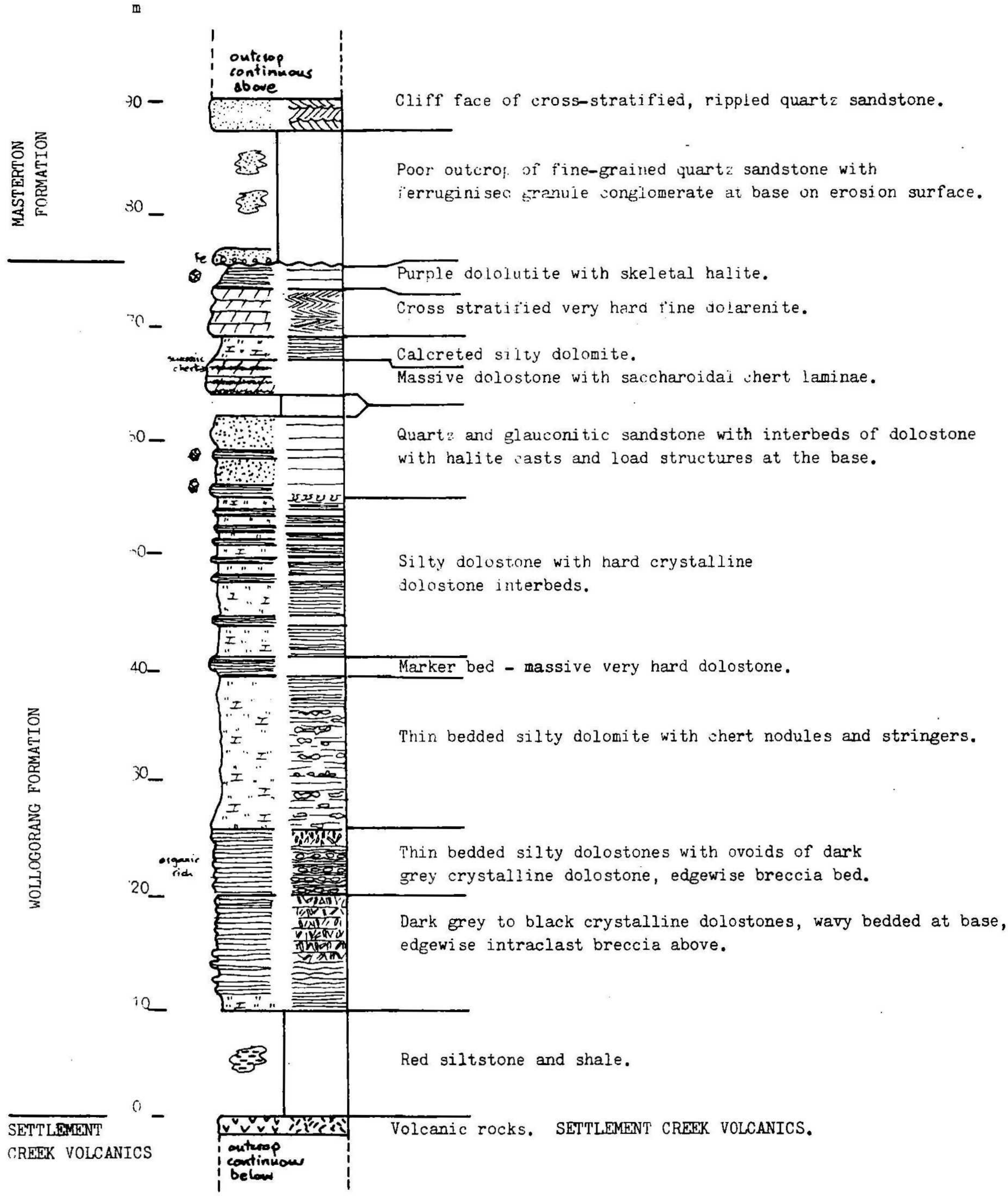


FIGURE 14 KILGOUR 78/9

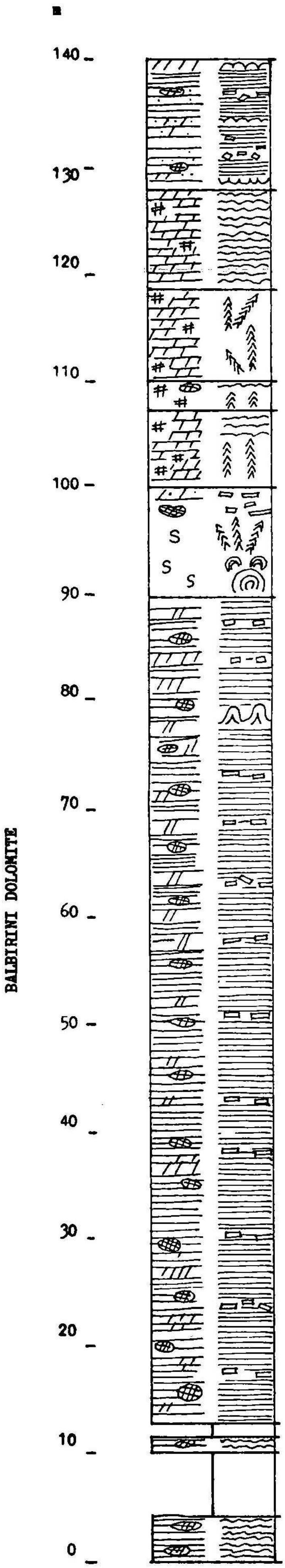


Thinly interbedded dololutite and dolarenite.
Small cuspate stromatolites and intraclasts.

Recrystallised dolarenite with relict sedimentary structures.

Branching Conophyton alternating with small vertical columnar Conophyton.

Vertical Conophyton with small cuspate stromatolites.

Vertical Conophyton in recrystallised dolarenite.

Dolarenite, intraclasts, and dololutite with chert nodules.

Conophyton complex (now Balbirina prima).

Teepees.

Alternations of quartz-rich dolarenite with intraclast breccia
and flat-laminated dololutite with chert laminae and nodules.

Cherty dololutite with stratiform stromatolites.

Cherty dololutite with stratiform stromatolites.

40

FIGURE 15a MALLAPUNYAH 78/1 (1)

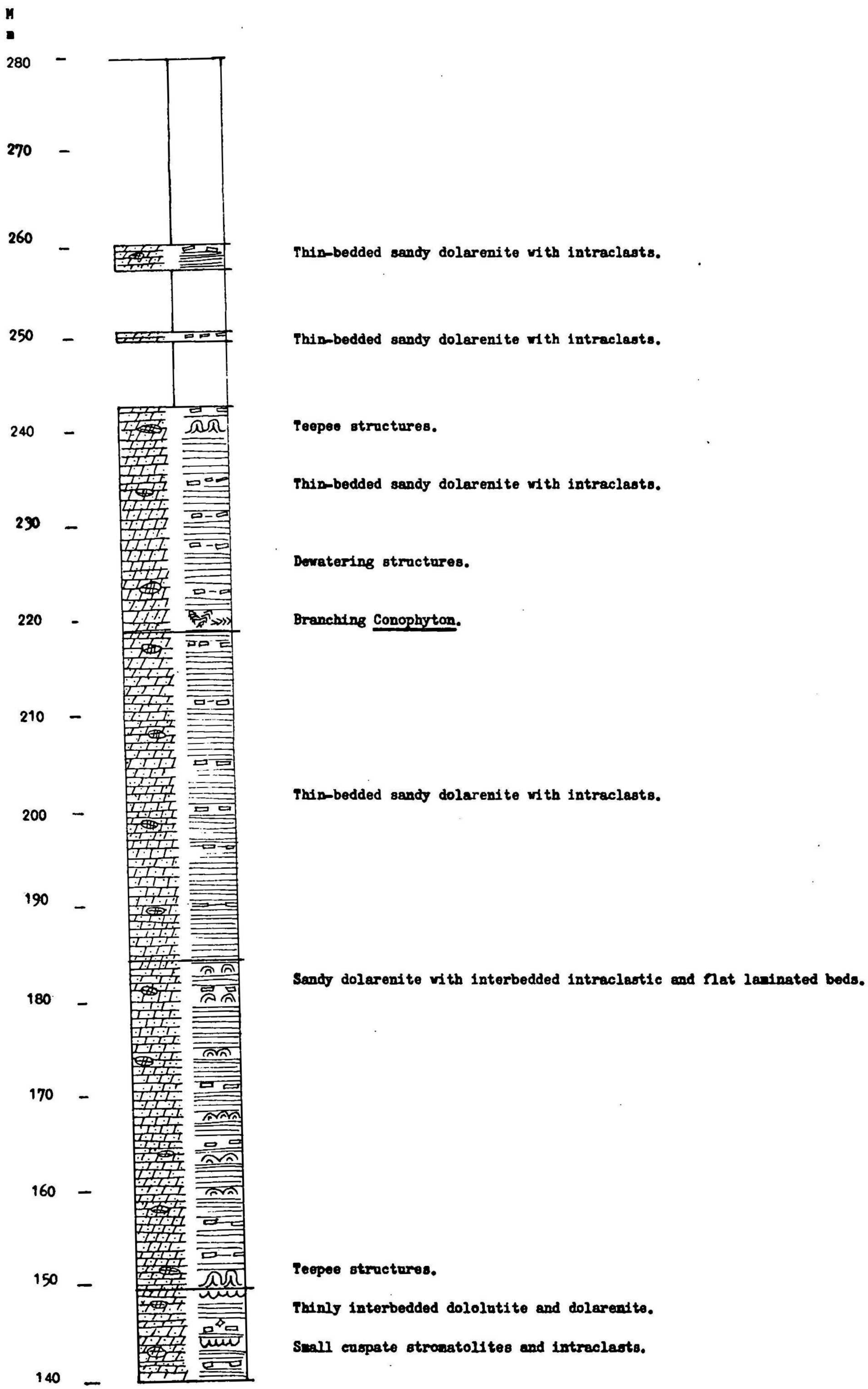


FIGURE 15b MALLAPUNYAH 78/1(2)

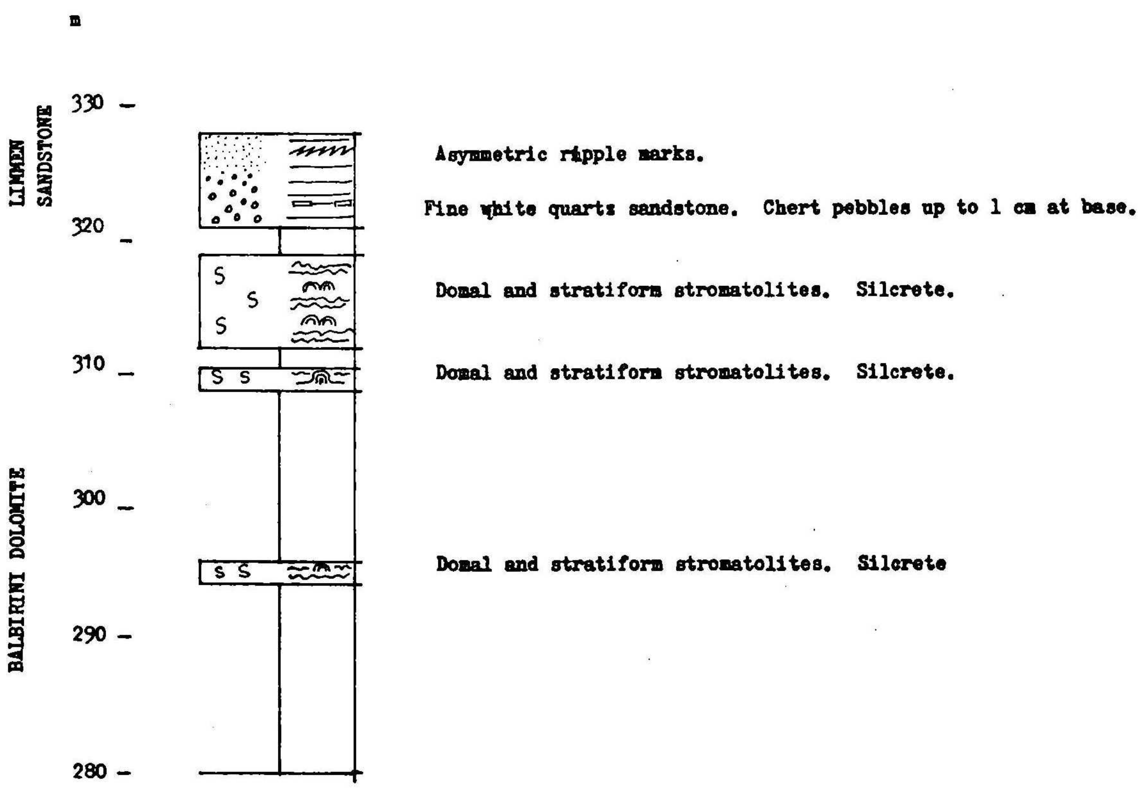


FIGURE 15c MALLAPUNYAH 78/1 (3).

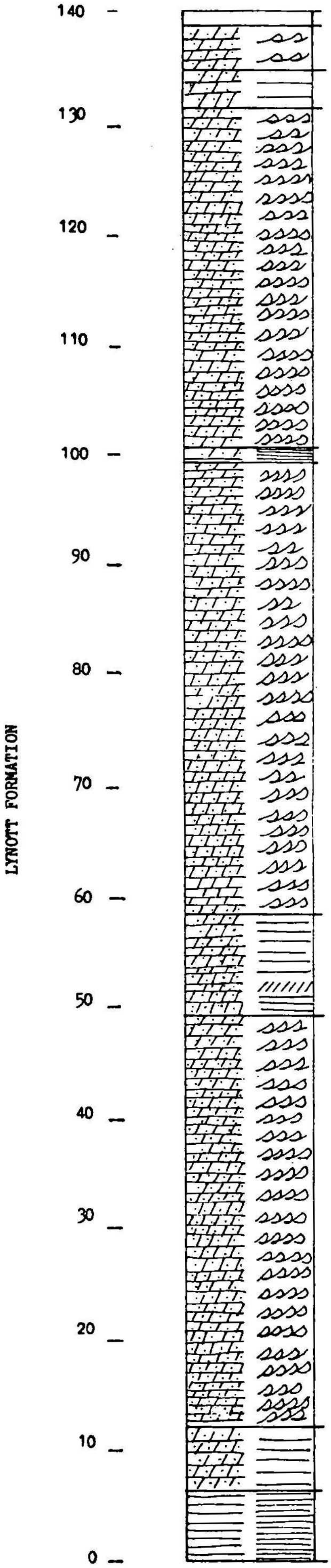


Thin-bedded dolarenite with slumping and dewatering.

Massive-bedded dolarenite.

Thin-bedded quartzose dolarenite with slumping and dewatering.

Very thin-bedded interbedded dolarenite and dolorudite.

Thin to fine-bedded sandy dolarenite. Bedding wavy and slumped. Overturned in easterly direction.

Massive-bedded quartzose dolarenite. Clasts of current-bedded sandy dolarenite.

Thin to fine-bedded sandy dolarenite. Bedding wavy and slumped producing low amplitude kink folds. Dewatering channels along axes of kink folds.

Massive-bedded quartzose dolarenite. Clasts of current-bedded sandy dolarenite.

Massive -bedded quartzose dolarenite.

Fine-laminated, flat-bedded carbonaceous dololutite.



FIGURE 16a MALLAPUNYAH 78/2 (1).

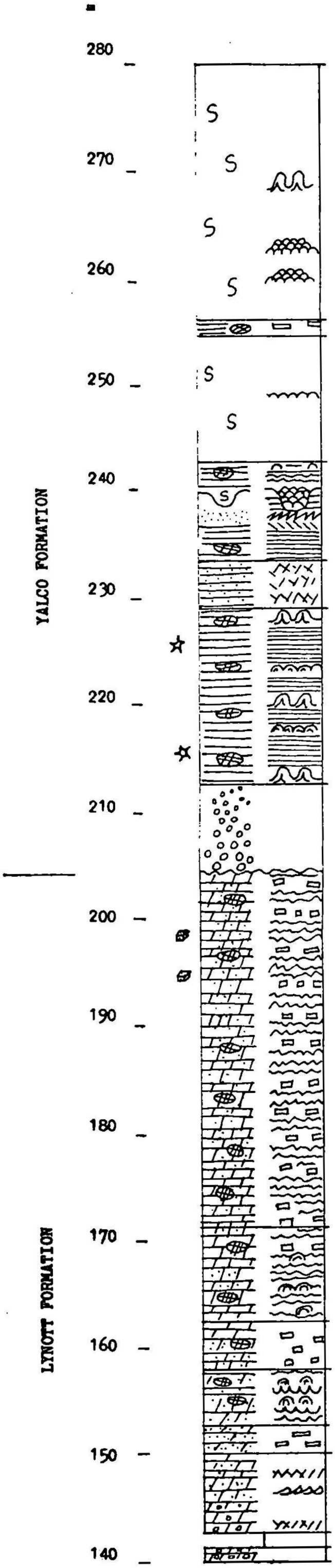


Teepee structures. Silcrete.

Small columnar stromatolites.

Small columnar stromatolites.

Fine-grained cherty dololutite with intraclasts.

Small domal stromatolites.

Bioherm of branching columnar stromatolites cross-cutting normal laminae.

Thin-bedded cherty dololutite. Thin-bedded quartz sandstone with climbing ripples.

Fine-grained dolomitic sandstone with herring-bone cross beds.

Thin-bedded cherty dololutite, abundant small stromatolites, teepees and polygons, desiccation cracks.

Unbedded conglomerate fining upwards. Cobbles up to 40 cm.

UNCONFORMITY

Dolarenite with chert lenses, quartz sand and intraclasts. Stratiform stromatolites.

Low domal and stratiform stromatolites. Sand disappears at top of unit.

Sandy dolarenite with dololutite intraclasts.

Small cuspate stromatolites interbedded with domal stromatolites.

Sandy dolarenite with dololutite intraclasts.

Dolomitic sandstone grading up into sandy dolarenite. Some low-angle cross-bedding. Minor slumping.

Massive-bedded pebbly dolorudite.



FIGURE 16b MALLAPUNYAH 78/2 (52).

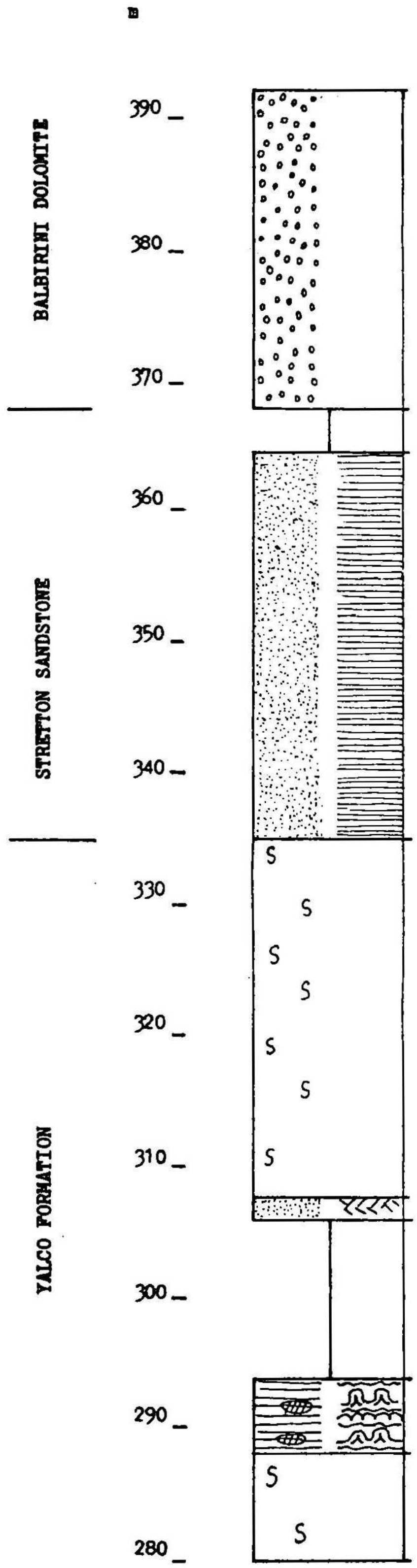


Massive conglomerate. Cobbles up to 20 cm diameter. Largely silicified.

Scattered sandstone fragments. UNCONFORMITY

Fine-grained green sandstone. Thin-bedded, some clay clasts, distorted mud-cracks. Fine-scale cross-bedding.

CONFORMABLE CONTACT

Poorly exposed silcrete of Yalco Formation.

Fine-grained cross-bedded sandstone.

Silcrete rubble.

Cherty dololutite. Teepees and polygons. Small anastomosing domal stromatolites.

Silcrete rubble.

FIGURE 16c MALLAPUNYAH 78/2 (3).

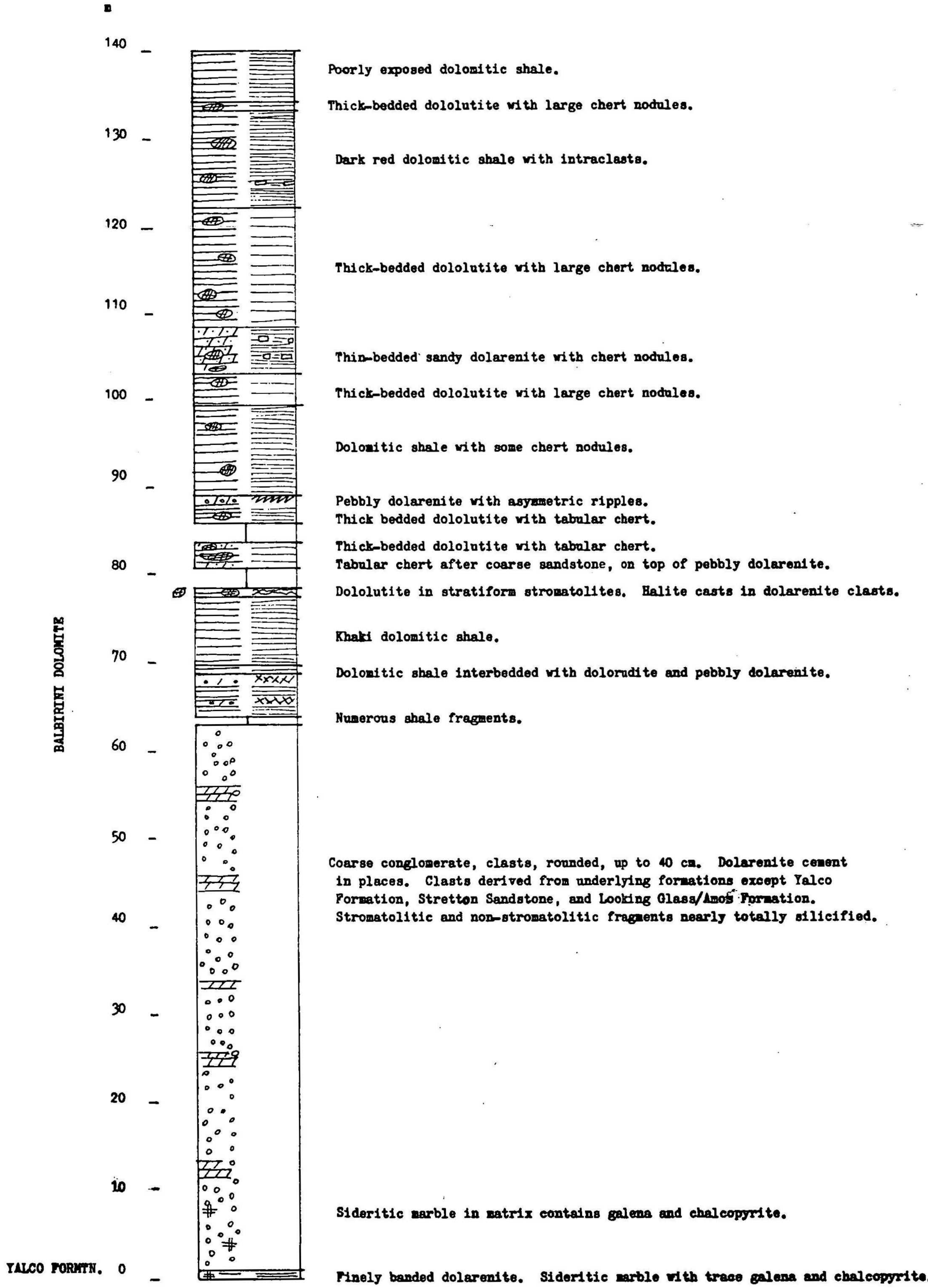


FIGURE 17a MALLAPUNYAH 78/3 (1).

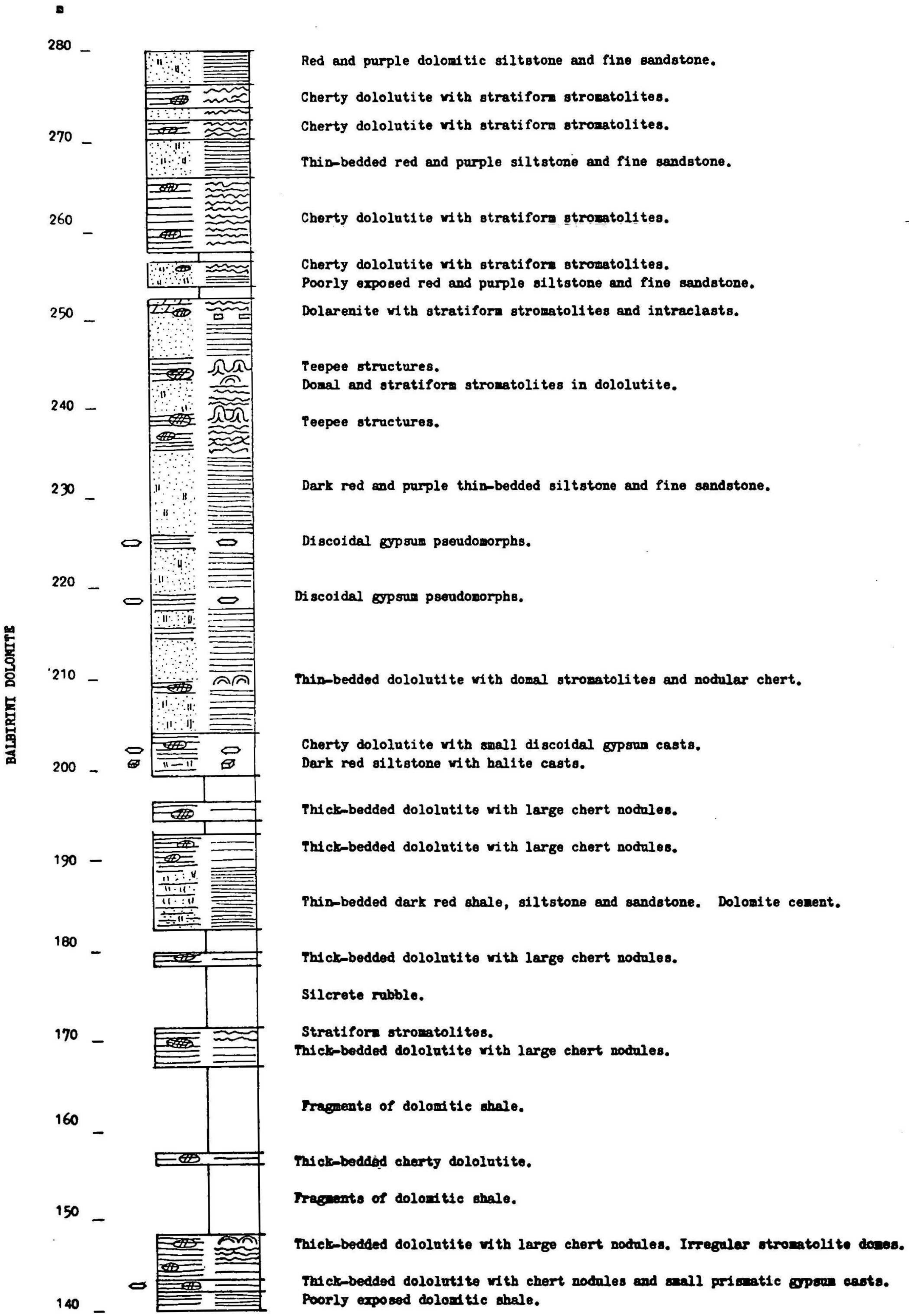




FIGURE 17b MALLAPUNYAH 78/3 (2).

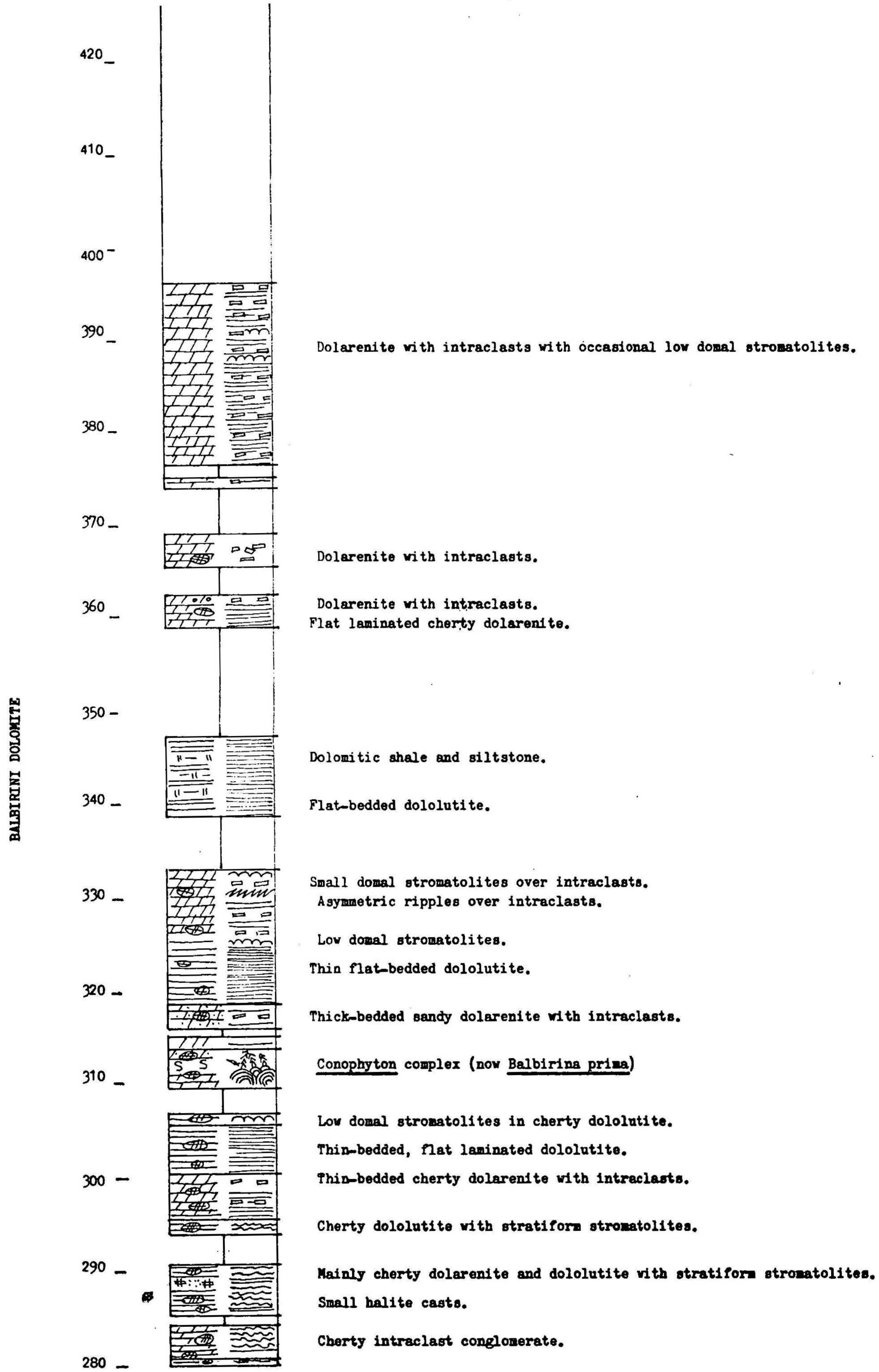




FIGURE 17c MALLAPUNYAH 78/3 (3).

LYNOTT FORMATION
(LOWER PART)

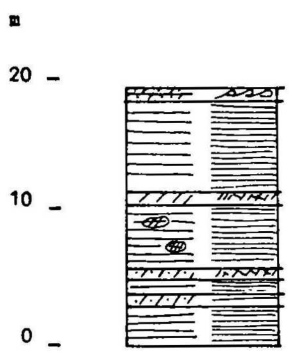


Remainder of section folded and faulted.

Slumped dolarenite.

Dolomitic shale.

Cross-bedded dolarenite.

Dolomitic shale with lenses of dolarenite.

Dolomitic shale with cross-bedded dolarenite at top.

Thin dolarenite bands.

Dolomitic shale.

FIGURE 18 MALLAPUNYAH 78/4.

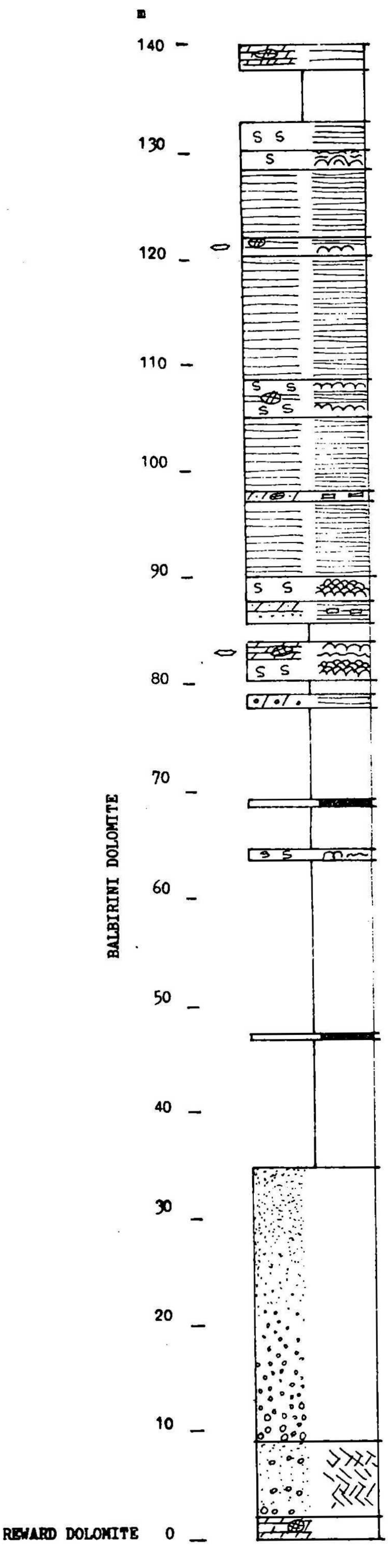


Thick-bedded dolarenite with nodular and bedded chert.

Flat-bedded dolarenite. Silcrete.
Irregular domal and stratiform stromatolites

Red and purple dolomitic shale.

Thick-bedded dololutite with chert nodules. Rare columnar and domal stromatolites. Six-sided pseudomorphs after gypsum.

Poorly exposed red and purple dolomitic shale.

Domal and stratiform stromatolites with interbedded dolomitic shale.
Iron pan at 107.

Red and purple dolomitic shale.

Thick-bedded cherty dolarenite. Quartz sand grains and intraclasts.

Red and purple dolomitic shale.

Slightly divergent irregular columnar stromatolites.
Quartz dolarenite with intraclasts and interbedded dolomitic shale.

Calcrete on shale.
Ferroan dolomite with chert nodules and prismatic gypsum pseudomorphs.
Columnar and domal stromatolites. Silcrete. Calcrete on shale.
Dolarenite with laminar and nodular chert.

Shale fragments and silcrete rubble.

Pink 'tuffite' bed.

Small domal and stratiform stromatolites. Silcrete.

Shale fragments and silcrete rubble.

Pink'tuffite' bed.

Boulders decrease in size up to 3 cm.

Pebble to boulder conglomerate, little apparent bedding. Boulders up to 15 cm include flat laminated and stromatolitic silicified carbonates, sandstone and chert.

Fine to medium grained quartz sandstone with chert pebble conglomerate. Low angle, small scale cross beds.

Massive dolarenite breccia. Karstic features.



FIGURE 19a MALLAPUNYAH 78/5 (1).

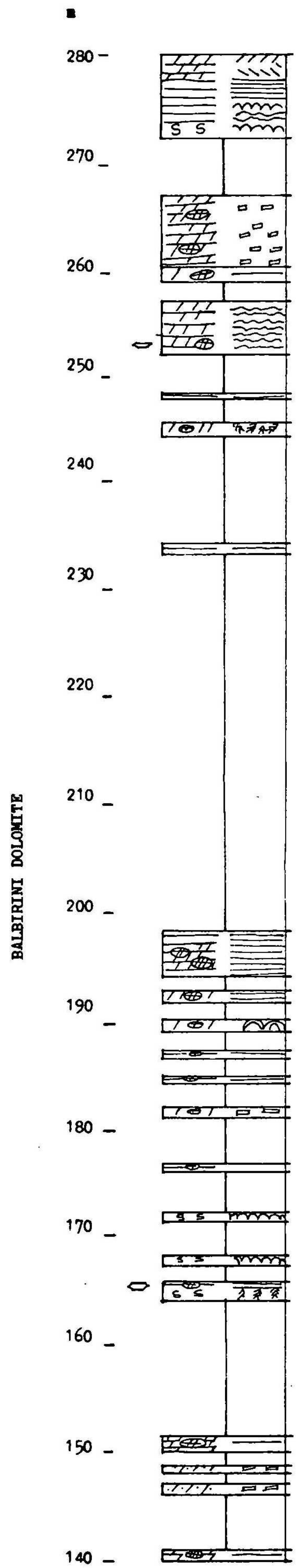


Cross-bedded dolarenite.
Dolomitic shale.
Domal stromatolites. Silcrete.

Thick-bedded dolarenite with abundant fine-grained intraclasts.
Massive pink dolarenite.

Dolarenite with chert nodules and stratiform stromatolites.
Discoidal gypsum casts.

Thin bedded dololutite.
Small irregular branching Conophyton.

Thick bedded dololutite.

Botryoidal quartz nodules.
Thin bedded dolarenite and dololutite.
Thin bedded dolarenite with nodular chert.
Dolarenite with large domal stromatolites.
Dololutite with chert nodules and layers.
Dololutite with chert nodules and layers.

Dolarenite with chert nodules and layers. Intraclasts.

Thick bedded dolarenite with chert nodules.

Small irregular domal stromatolites. Silcrete.

Small domal stromatolites. Silcrete.

Flat-bedded dololutite with chert laminae. Six-sided gypsum pseudomorphs. Vertical Conophyton.

Silcrete rubble.

Thick-bedded dolarenite with nodular and bedded chert.
Thick-bedded dolarenite with quartz sand and intraclasts.

Thick-bedded dolarenite with nodular and bedded chert.

FIGURE 19b MALLAPUNYAH 78/5 (2).

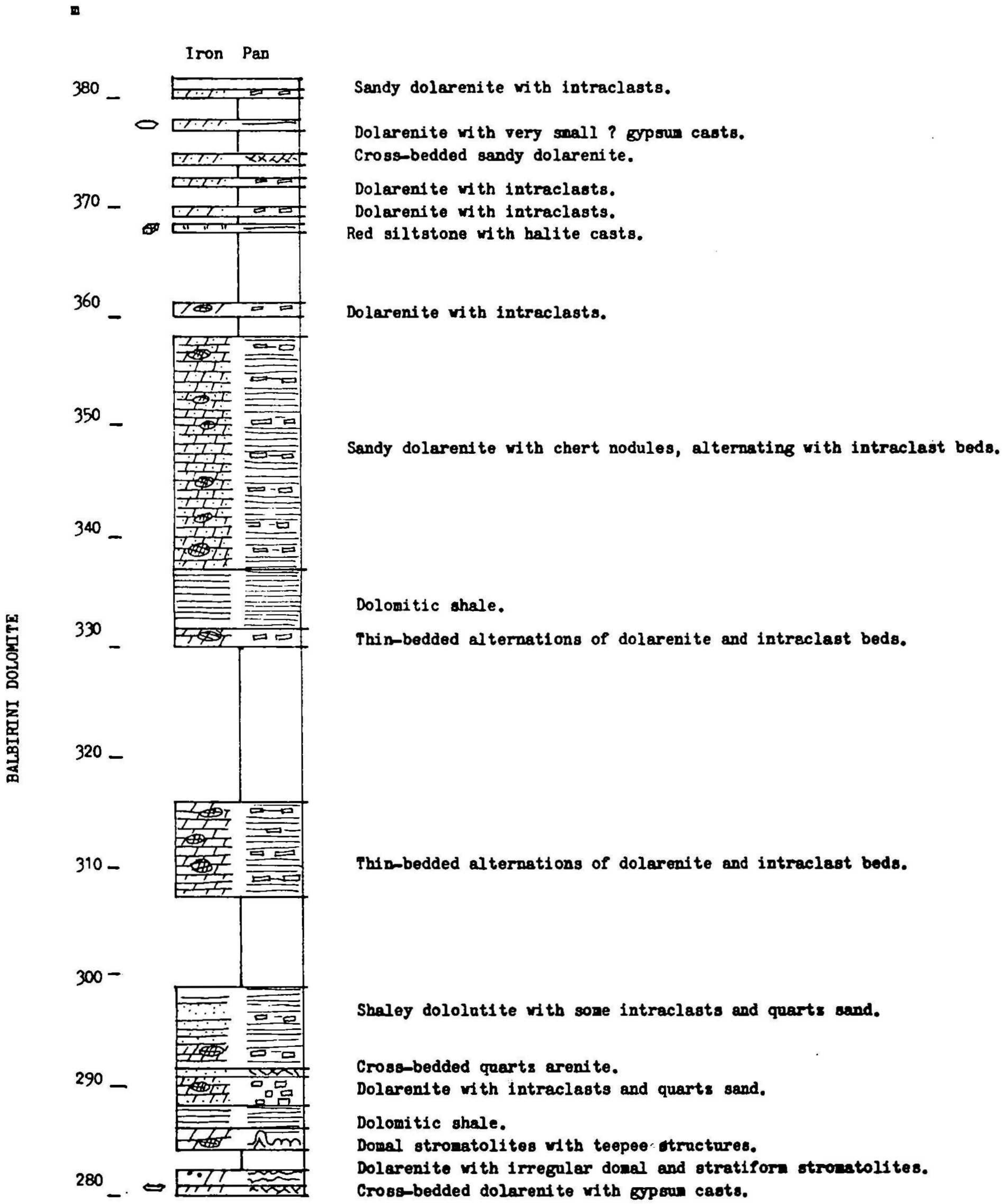


FIGURE 19c MALLAPUNYAH 78/5 (3).

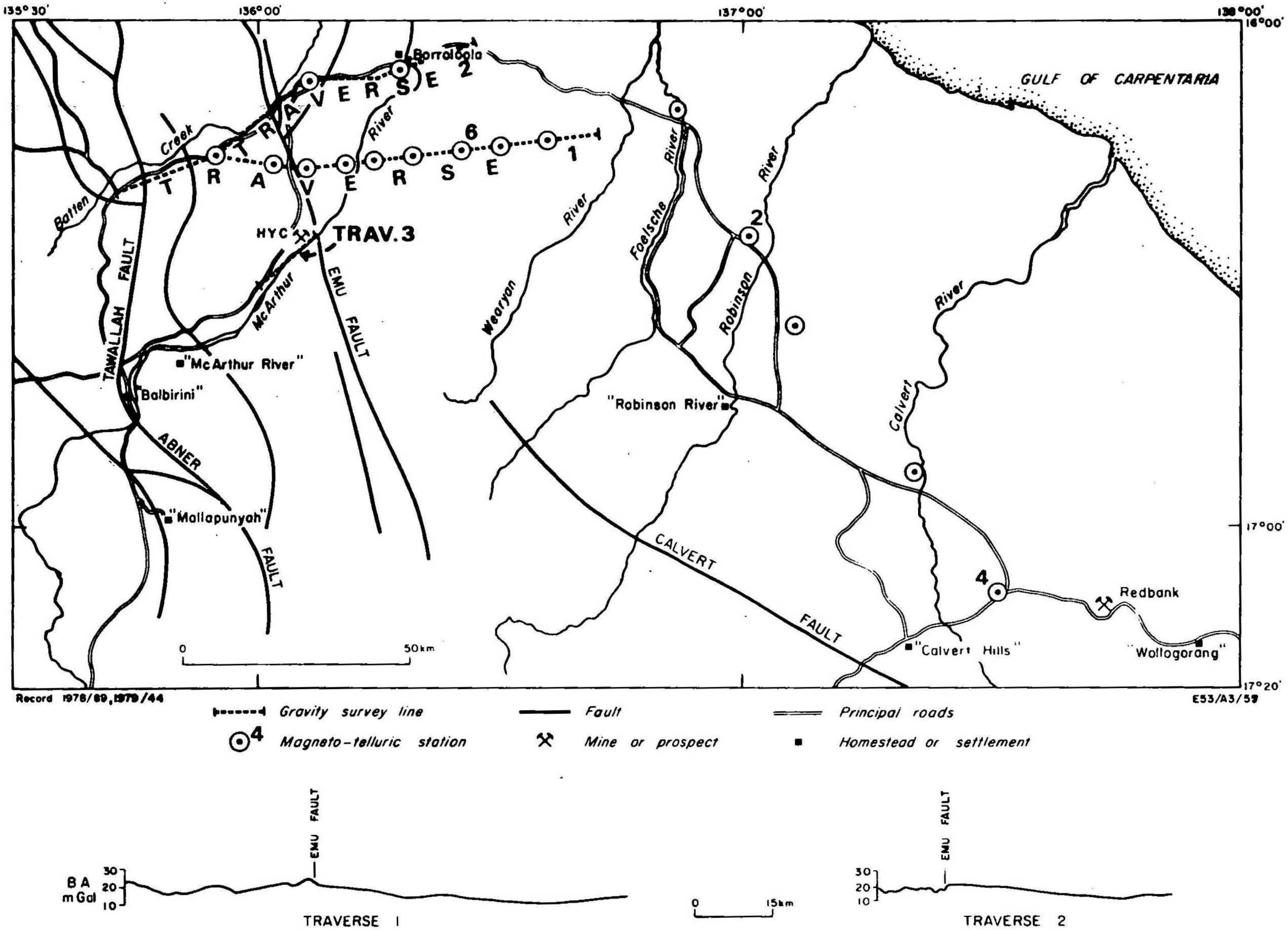


Fig. 20 Locality map and preliminary Bouguer anomaly profiles — McArthur Basin magneto-telluric and gravity survey, 1978.
(From Record 1979/15)

57

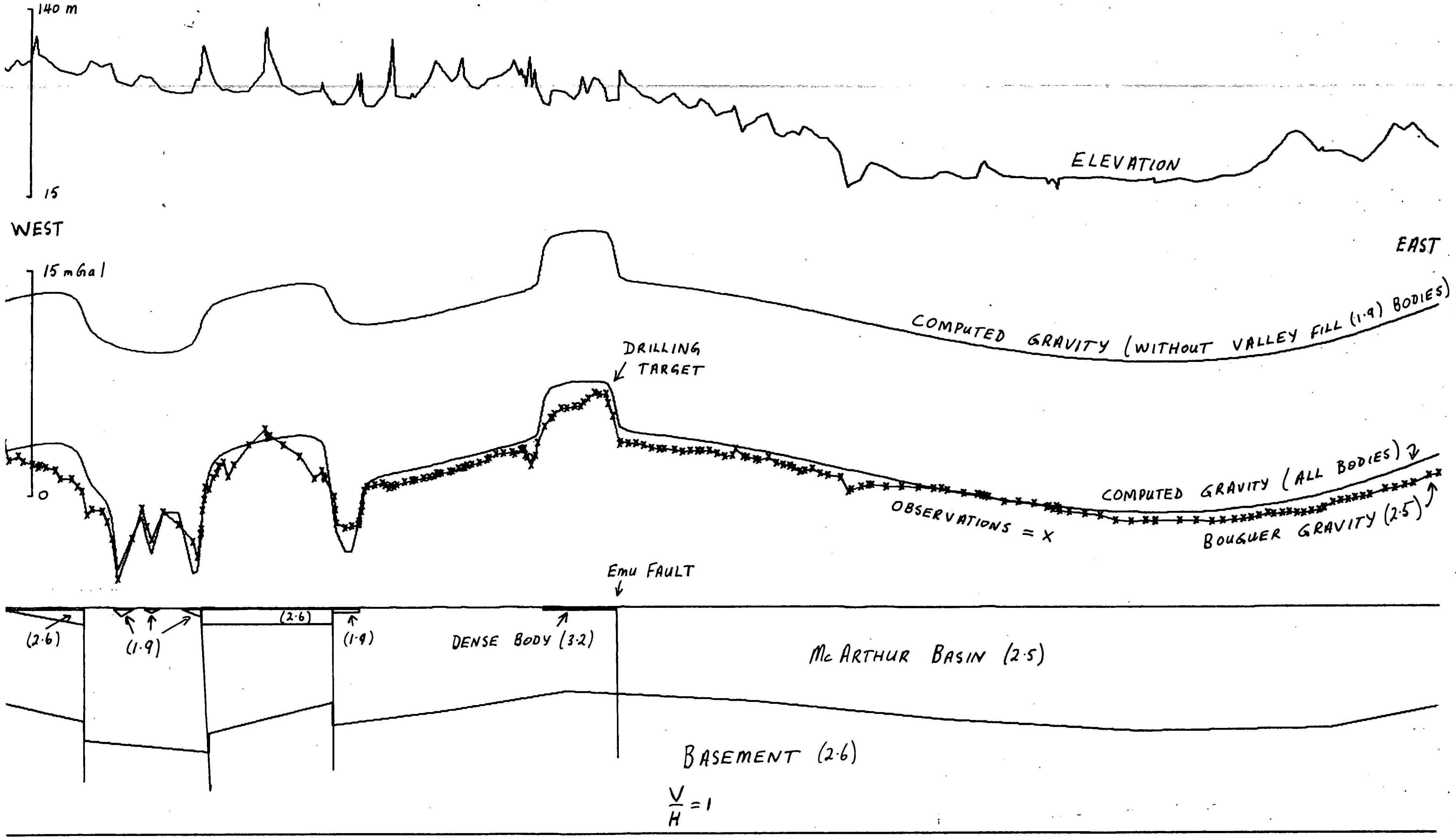


FIGURE 21. BOUGUER GRAVITY AND INTERPRETATION ALONG TRAVERSE 1.

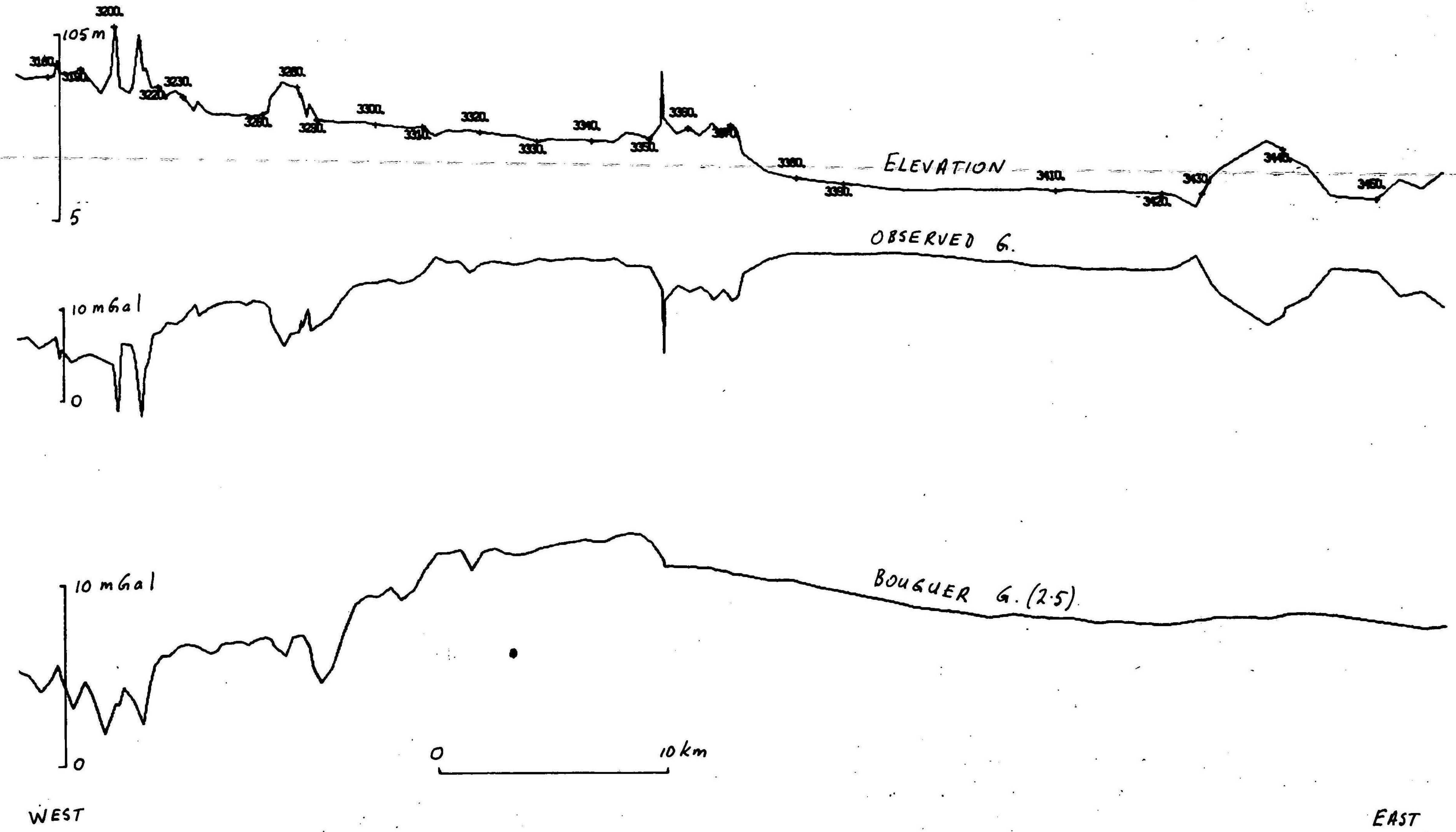


BOUGUER GRAVITY ALONG TRAVERSE 2

FIGURE 22.

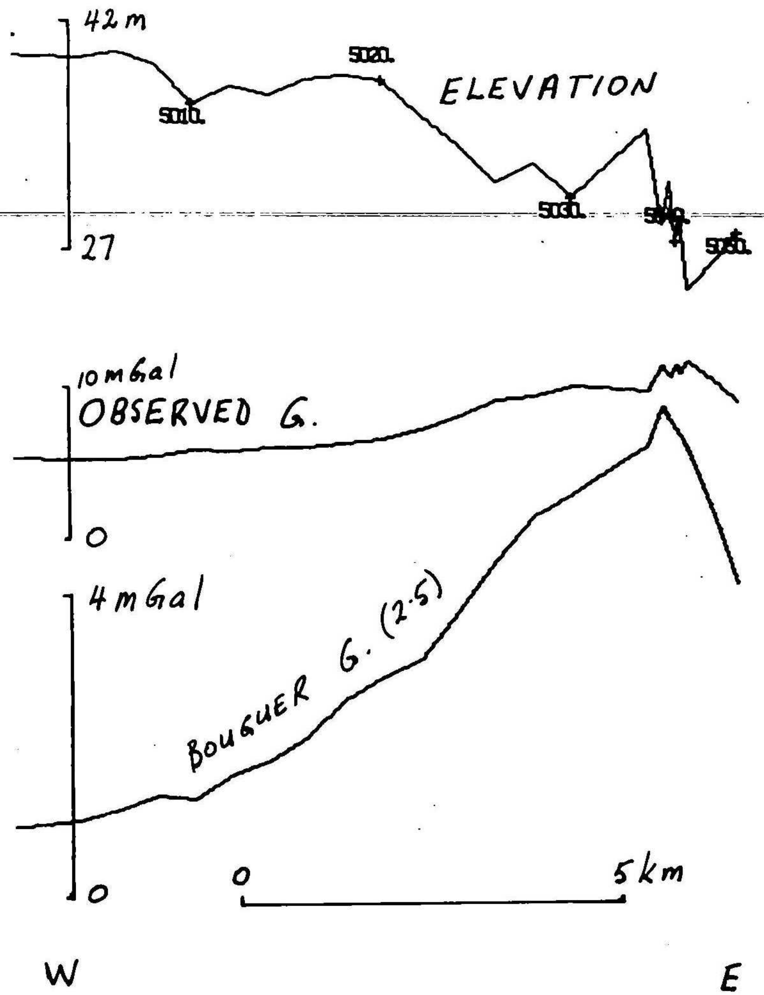


BOUGUER GRAVITY ALONG TRAVERSE 3

FIGURE 23.

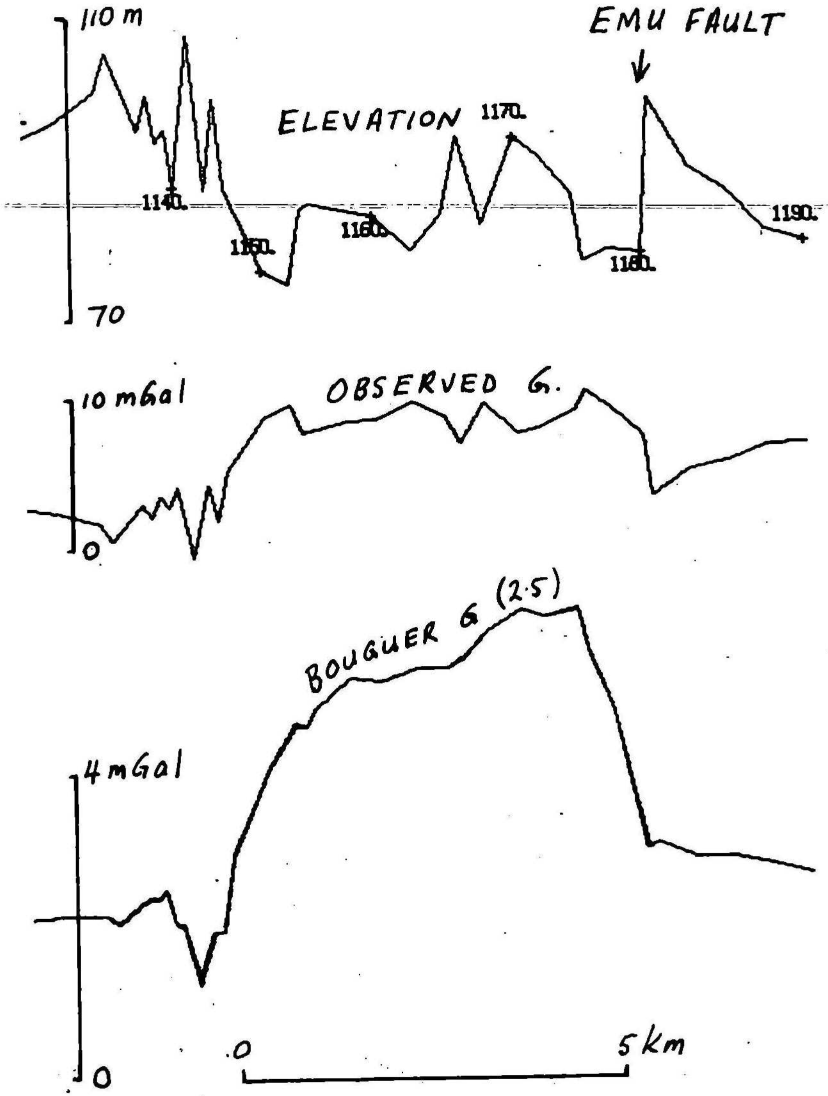


PART OF TRAVERSE 1.

FIGURE 24.